12-1-1996

Mercury Sorption on Metal Oxides

Heidi L. Hitchcock

MERCURY SORPTION ON METAL OXIDES

by

Heidi L. Hitchcock
Bachelor of Science in Chemical Engineering
University of North Dakota, 1995

A Thesis

Submitted to the Graduate Faculty

of the

University of North Dakota

in partial fulfillment of the requirements

for the degree of

Master of Science

Grand Forks, North Dakota
December
1996

The thesis, submitted by Heidi L. Hitchcock in partial fulfillment of the requirements for the Degree of Master of Science from the University of North Dakota, has been read by the Faculty Advisory Committee under whom the work has been done and is hereby approved.

Douglas Leedlan
(Chairperson)

Brian Young

Edwin A Olson

John Arthur Murrell

The thesis meets the standards for appearance, conforms to the style and format requirements of the Graduate School of the University of North Dakota, and is hereby approved.

Harvey Knull
Dean of the Graduate School

12-4-96
Date

PERMISSION

Title Mercury Sorption by the Constitutive Metal Oxides in Fly Ash

Department Chemical Engineering

Degree Master of Science

In presenting this thesis in partial fulfillment of the requirements for a graduate degree from the University of North Dakota, I agree that the library of this University shall make it freely available for inspection. I further agree that permission for extensive copying for scholarly purposes may be granted by the professor who supervised my thesis work or, in his absence, by the chairperson of the department or the dean of the Graduate School. It is understood that any copying or publication or other use of this thesis or part thereof for financial gain shall not be allowed without my written permission. It is understood that due recognition shall be given to me and to the University of North Dakota in any scholarly use which may be made of any material in my thesis.

Signature Heidi Hutchcock

Date December 3, 1996

TABLE OF CONTENTS

LIST OF ILLUSTRATIONS

LIST OF TABLES

ABSTRACT

This project addresses the fundamental aspects of toxic metal (mercury) sorption by metal oxides. The emission of toxic trace elements from anthropogenic sources, such as combustion, has drawn attention to potential dangers for the ecosystem. Particular concern has been directed toward mercury species because of their high toxicity and tendency to convert into forms leading to mercury accumulation in mammals. Efforts to control mercury species release have centered on sorption technology using carbonaceous sorbents. However, it has been found, in some cases, that fly ash also has some sorptive properties towards mercury species. In order to further understand the sorption processes in the fly ash, a project was initiated to study the mercury sorption properties of various metal oxides. The purpose of the project was to serve as a baseline for further fly ash studies by determining differential sorption capacities of fly ash types. Along with the metal oxides studies, an assortment of fly ashes were looked at.

Some of the metal oxide species (Al_2O_3) have no sorption properties for Hg. On the other hand, other metal oxides can oxidize the Hg^0 or catalyze the air oxidation of Hg^0 to form HgO. If SO_2 or HCl are present in the flue gas, a mercury salt can form. A parametric study was undertaken of the effects of condition variables such as temperature and air on the sorption of mercury on metal oxides. The investigation began with simple oxides and proceeded to more complex mixed oxides and other transition or lanthanide

metal oxides. Elemental mercury (Hg^0) mass uptake efficiency of the oxides was monitored using a continuous mercury vapor monitor. Infrared spectrophotometry was used to characterize the oxides before mercury uptake experiments to achieve a better understanding of the binding interactions that determine the sorption process for each mercury species.

The determination was made that molecular oxygen is not involved in the reaction of supports with elemental mercury. The reaction, therefore, is not catalytic.

Chemical activation of supports (Al_2O_3 and carbon) increased their adsorption capacity. For example, Al_2O_3 alone emitted 84 % Hg into the effluent; after activation with MnO_2, no trace (0 %) Hg was emitted into the effluent.

Several iron oxides were tested; active samples were less dense than inactive samples. Active samples, like maghemite, include vacant sites. Vacancies in the iron oxide structure make it possible for Hg to be oxidized by iron species on the inside of the structure.

All but one fly ash failed as sorbents for Hg. Fly ashes are inactive due to the iron species which are heated to high temperatures. The iron forms hematite which is inactive.

ACKNOWLEDGMENTS

I want to express my sincere thanks to the my advisor, Doug Ludlow. His guidance and assistance was appreciated. I would also like to thank the other members of my committee, Jim Newell, Ed Olson, and Brian Young. Jim was kind enough to take on more responsibility and make me part of his research group after Doug moved to Missouri. I would also like to thank Ed for supervising my research and answering my questions.

I am also grateful to The Associated Western Universities for awarding me with a fellowship.

Lastly, I would like to thank my parents and brother for their moral support when everything wasn't quite going the way I hoped. I am also very grateful for parents financial assistance.

To My Parents,

Chuck and Sue Hitchcock

CHAPTER I

INTRODUCTION

The emission of toxic trace elements from combustion has drawn attention to potential dangers for the ecosystem. During combustion processes, mercury can vaporize and condense and/or undergo speciation change. Mercury is sorbed on the surface of the fly ash particles, usually oxides. These particles are hard to remove from stack gases using current collection devices and mercury pollution is released in the flue gases from plant stacks. Particular concern has been directed toward mercury species because of their high toxicity and tendency to convert into forms leading to mercury accumulation in mammals.

Mercury can be removed from a flue gas stream by three processes: physical adsorption, chemisorption, or amalgamation. Mojtahedi and Mroueh define physical adsorption as when the reactant is attracted by surface or van der Waals forces (responsible for the nonideal behavior of gases). Chemisorption involves chemical bonds which arise from an actual sharing and donation of electrons; the forces being of the same order of magnitude as those in chemical reactions.(Mojtahedi and Mroueh, 1989) Amalgamation occurs when mercury reacts with a metal to form a metal alloy.(Ebbing and Wrighton, 1990)

Activated carbons adsorb a few hundred micrograms to a few milligrams of mercury primarily by physisorption. For maximum physisorption to take place, operation

must be maintained below 100°C. For temperatures up to 200°C, activated carbon will adsorb most mercury (II) chloride; but, it does not adsorb all forms of mercury.(Metzger and Braun, 1987)

It has been found that activated carbons that have been chemically treated with iodine, sulfur, copper (II) chloride, or copper and zinc have a increased capacity for mercury. However, chemically impregnated activated carbons cost more and their usage has to be optimized for the specific application.

Most current inorganic adsorbents do not work well as mercury adsorbents when water vapor is present in the flue gas streams. Chemical impregnation increases their adsorption capacity and the adsorbent is no longer affected unfavorably by water vapor.(Mojtahedi and Mroueh, 1989) One plausible explanation for this phenomena is that the physisorption principle is operating, and the water is competing for sites with the mercury. If the carbon sorbents are chemically treated to introduce chemisorption sites specifically for mercury species, the effect of water vapor adsorption is minimized.

Inorganics like clay and zeolites have a low cost and are readily available; but, adsorption can only occur at the microgram level at room temperature. At high temperatures, oxygen needs to be present for significant adsorption to take place with chabazite, a type of zeolite. This effect may be due to chemical oxidation of the surface, allowing the appropriate interaction with mercury.(Mojtahedi and Mroueh, 1989)

Several adsorbents adsorb mercury by amalgamation. Silver/4A molecular sieves remove Hg and moisture from gases. They are also regenerable and have long term stability.(Yan, 1994) Mercu-Re manufactured ADA Technologies, Inc., contains noble

metals that capture Hg and recycle it. Mercury removal efficiencies are greater than 90 percent.(Caruana, 1996)

It has been found, in very limited cases, that fly ash has some sorptive properties towards mercury species. Some of the metal oxide species (Al_2O_3) have no sorption properties for Hg^0. On the other hand, other metal oxide fly ash constituents could oxidize Hg^0 to form HgO or a mixed metal oxide; the ability of fly ash to adsorb mercury may be due to this.

There are several metal oxides in fly ash. A majority is mullite, an alumina silicate. Other aluminum silicates include: gohlenite, anorthite, and albite. Fly ash also includes spinel, a dense iron aluminum silicon; quartz, SiO_2; calcium minerals; hemaite, an iron oxide; spinel, $MgFe_2O_4$; and opal.

In order to further understand the sorption processes in the fly ash, a project was initiated to study the mercury sorption properties of various metal oxides. The objectives of this research are to evaluate the potential for the adsorption of elemental mercury vapor on inorganic oxide materials, determine which metal inorganic oxides can catalyze the oxidation of elemental mercury, and ascertain the nature of the sorption process by examing temperature effects and oxygen requirements. This goal will assist in understanding flue gas treatment processes and has the potential to provide process information for controlling mercury emissions.

CHAPTER II

LITERATURE REVIEW

This chapter covers the literature review in two sections: Mercury Pollution and Mercury Control Technologies. The review of mercury pollution will address the toxicity of mercury and its progression up the food chain leading to adverse effects on humans. Control technologies will include aqueous scrubbers and solid adsorbents such as carbon and inorganic adsorbents.

Mercury Pollution

Mercury is listed third on the Environmental Protection Agency's list of 89 toxic substances.(Caruana, 1996) The principal anthropogenic sources of mercury emissions are coal combustion, smelting, and incineration. These sources contribute 30-75 percent of the total yearly addition of mercury to the environment, amounting to 25,000 to 150,000 tons per year compared to 20,000 tons per year from other human activity.(Von Burg, 1995) Several large countries (e.g. China, India, Brazil) are undergoing rapid industrialization and could quickly increase mercury emissions to the atmosphere from coal consumption in the future.(Prestbo and Bloom, 1995)

Mercury has a high toxicity and tendency to convert into forms , e.g. methyl mercury, leading to mercury accumulation in mammals. Mercury is released in the flue gases from plant stacks and can exist in the environment in the form of elemental mercury,

inorganic mercury salts or oxides, or organomercury compounds. Mercury in the air can then become deposited in the soil and water. The half-life of mercury in air is estimated to be about one year.(Von Burg 1995) Mercury in soil can adsorb onto organic matter. Adsorbed mercury cannot be released until decay processes take place. Mercury in water can settle into sediment or be adsorbed by suspended particulate matter. Terrestrial and aquatic plants then uptake the mercury into their roots, stems, leaves, and flowers or fruit depending on how the plant is exposed to the mercury (air, soil, etc.).

The next step in the food chain is consumption of the plants by aquatic life or humans. The number one source of non-occupational exposure to mercury is ingestion of mercury containing food, especially fish and other seafood.(Von Burg, 1995) Mercury has a tendency to accumulate in biota and large fish and is considered the most serious environmental threat to fish and wildlife in the southwestern United States.(Constantinou, *et al.*, 1995) The mercury concentrations are higher than the acceptable limits and fish consumption advisories have been issued in all ten southwestern states.(Dvonch, *et al.*, 1995) Seventy percent of all U.S. fish consumption advisories issued relate to mercury. The amount of mercury in fish is increasing at the rate of three and a half percent per year in some lakes.(Shell and Anderson-Carhahan, 1995) The consumption of these fish have proven detrimental to reptiles, birds, and mammals (including humans). Effects of mercury accumulation include inability to reproduce, hair loss, nervous disorders, and mortality.(Facemire, *et al.*, 1995)

Because of the significant adverse effects of mercury accumulation in the ecosystem, stricter regulations regarding mercury emissions have been put in place. The

regulation of hazardous air pollutants, including mercury, was significantly revised by the 1990 Clean Air Act.(Zeugin, *et al.*, 1994) The Occupational Safety and Health Act; The Food, Drug, and Cosmetic Act; and The Clean Water Act also regulate the emission of mercury.

Mercury Control Technology

During combustion processes, mercury vaporizes, may undergo a change of valence state, and then condenses out as flue gas cools. The condensation can be homogeneous forming a fume or heterogeneous by adsorbing on the surface of ash particles. Heterogeneous condensation predominates when a surface is present and will usually occur on the smallest particles. The core of these particles are metal oxides which have heavy metals, such as mercury, on the surface. These particles are not easily removed from stack gases using current collection devices like electrostatic precipitators (ESPs) and baghouses. Therefore, the gases escape into the atmosphere taking the captive mercury species. Although there is only a small amount of mercury in coal (e.g. 0.07 to 0.28 μg Hg/g coal), it is estimated that 90 percent of it is released into the environment after burning.(Fang, 1978 and U.S. Department of Energy, 1996)

There are three techniques for mercury removal: physical adsorption, chemisorption, and amalgamation. Physical adsorption is the attraction of the reactant by the surface or by van der Waals forces.(Mojtahedi and Mroueh, 1989) Chemisorption involves quasi chemical bonding arising from the sharing of electrons with the forces being of the same order of magnitude as those in chemical reactions.(Majtahedi and Mroueh,

1989) Amalgamation is a solid solution process when mercury reacts with a metal to form a metal alloy.(Ebbing and Wrighton, 1990)

The behavior of mercury vapor in collection devices is not clearly understood because it exists in many forms including elemental mercury (Hg^0), divalent mercury (Hg(II)), such as mercury chloride ($HgCl_2$).(Schlager, *et al.*, 1995) Mercury also undergoes several complex interactions. Current cleaning systems can remove oxidized mercury including Hg(II); but, elemental mercury is still emitted.(Sappey, *et al.*, 1995) Studies performed by the U.S. Environmental Protection Agency's Research Division and the Utility Air Group in 1995 indicated that the removal of mercury is not consistent in electrostatic precipitators (ESP) or fabric filters. The mean removal efficiency at the temperatures encountered in these devices is thirty percent. The removal in a combined ESP and wet Flue Gas Desulfurization (FGD) systems is also inconsistent, with efficiencies ranging from zero to ninety percent. The mean removal efficiency was 45 percent.(Behrens and Chu, 1994) Current techniques for mercury emissions are difficult, time consuming, and expensive.(Sappey, *et al.*, 1995) Consequently, there exists a need for the development of technology to decrease the amount of mercury released into the environment. In order to develop control technologies, we need a fundamental knowledge of the behavior of mercury.(Morency, *et al.*, 1994 and Otani, *et al.*, 1984) Presently, there is not a single cost-effective, reliable method for the collection of all mercury pollution species.(Caruana, 1996)

Two types of mercury control technologies that will be discussed are aqueous scrubbers and solid adsorbents. Solid adsorbents include activated carbons and inorganic compounds.

Aqueous Scrubbers

Wet scrubbers only work for water soluble compounds like mercury chloride ($HgCl_2$), not elemental mercury. The solubility of $HgCl_2$ is not high; but at low concentrations, $HgCl_2$ will go into solution. This is because lime is added to control the pH because sulfur converts Cl to an acid. A problem with using a wet scrubber for mercury control is that mercury is captured in the wet scrubber and becomes another hazardous waste disposal problem. Another problem with wet scrubbers is that their removal efficiency is inconsistent. The removal efficiency can be high at times and low to moderate at others depending on flue-gas conditions; coal burned; fly ash and gas composition; mercury speciation; or compound, sorbent, or scrubber properties.(Caruana, 1996)

Wet scrubbers have lower removal efficiencies than ESPs or fabric filters. They are also the least effective for very small particle sizes (<5μm). Wet scrubbers are the most common FGD system in coal-fired power stations. In the wet FGD unit, gaseous compounds condense on particles. There is a prescrubber that removes approximately sixty percent of the Hg(II) and the scrubber that removes approximately forty percent. There is warm enough air flow that Hg^0 is carried through the FGD systems as a vapor. There is nothing in the system to chemically oxidize/catalyze the Hg^0; hence, the Hg^0 cannot adsorb on anything for removal. Flue gases cool in the wet scrubber and allow

most volatile trace elements to condense. The outlet temperature of the scrubber is 50-60°C. Some mercury does remain in the flue gas.(Clarke, 1993)

Research conducted by the U.S. Environmental Protection Agency (EPA) Office of Research and Development (ORD) on particulate removal efficiencies of air pollution control systems (APCSs) indicated that removal efficiencies of mercury from wet scrubbers ranged from 67 to 99 percent. The average removal efficiency was 87 percent. The removal efficiencies decrease with lower inlet concentrations.(Carrol and Thurnau, 1994)

Solid Adsorbents

Solid adsorbents will be classified into two categories: activated carbons and inorganic compounds.

Activated Carbons

Activated carbons are widely used as adsorbents which are effective at low temperatures for physically sorbing pollutants or contaminated species. At temperatures of 100°C or greater, physical desorption is very rapid and the carbon does not work well as a sorbent. Impregnation with sulfur, iodide, or chloride ions increase the adsorption capacity of activated carbons. The impregnated species react with mercury to form a stable compound, i.e. chemisorption. Chemisorption reactions only produce stable compounds at temperatures below 200-300°C. Nonetheless, activated carbons only adsorb a few hundred micrograms to a few milligrams of heavy metals like mercury depending on speciation of Hg, the type of activated carbon used, and reaction conditions.(Mojtahedi and Mroueh, 1989)

For temperatures up to 200°C, activated carbon can adsorb most mercury (II) chloride contained in the gas stream.(Metzger and Braun, 1987) Several activated carbons have been used for the removal of mercury. These include coconut shell, hardwood, and low-rank coals which have been thermally, steam, or chemically activated. However, it can not be used for extracting total mercury or for adsorbing specific forms of mercury due to the loss of impregnation material by vaporization or the formation of volatile compounds when the adsorbent is used at elevated temperatures.(Mojtahedi and Mroueh, 1989) Iodized activated carbon is an excellent adsorbent for metallic mercury and mercury (II) halogenides in an air stream for temperatures up to 180°C.(Metzger and Braun, 1987)

Chemically impregnated activated carbons adsorbed several times more mercury(0) than do thermally activated carbons. Activated carbons impregnated with a chloride salt can adsorb up to three-hundred times as much mercury(0) as thermaliy activated carbons. For maximum mercury sorption to take place, operation must be maintained under 100°C.(Mojtahedi and Mroueh, 1989) However, chemically impregnated activated carbons are very expensive ($3-5 per pound) and their usage has to be optimized.

Inorganics

Many inorganic adsorbents are polar and preferentially adsorb water vapor over mercury from the flue gas stream. Water vapor is present in most flue gas streams and this limits the use of such adsorbents for mercury is ineffective. Chemical impregnation increases their sorption capacity. The impregnated compound reacts with mercury to form a stable mercury species. The chemisorption process is not detrimentally affected by

water vapor as is the case with physical adsorption. Water vapor adsorption may on occasion be favorable.(Mojtahedi and Mroueh, 1989) Seven types of inorganics will now be discussed.

Clays

The low cost and ready availability of clays make them attractive candidates for adsorbent use. They can adsorb mercury at the microgram level at room temperature.(Mojtahedi and Mroueh, 1989) They can also be used with other low cost materials like fly ash or limestone to yield a greater adsorption capacity than any of its original components.

Zeolites

Zeolites also have a low cost and are readily available but their tendency to preferentially adsorb water limits their use. They will adsorb mercury only if oxygen is present; otherwise, adsorption of mercury is minimal. Hence, the uptake of mercury is most likely due to a surface reaction with oxygen. The sorption capacity of zeolites is increased with sulfide or iodide impregnation. Nonetheless, zeolites must be used under 100°C for maximum mercury adsorption.(Mojtahedi and Mroueh, 1989)

Chabazite, a type of zeolite, can adsorb twenty-seven percent of its own weight in mercury.(Barrer and Whiteman, 1967) The mercury-chabazite complex can only be formed in the presence of oxygen. Again, this may indicate that the chabazite is working as a heterogeneous catalyst to catalyze the oxidation of mercury. Chabazite containing Ca^{++}, Na^{+}, and Pb^{++} can only adsorb a small amount of mercury. Mercury(Hg^{++})- and

silver(Ag^+)-rich chabazite are reduced during chemisorption to adsorb a larger amount of mercury.(Barrer and Whiteman, 1967)

The Medisorbon process uses a hydrophobic silica zeolite that is manufactured by Degussa AG. Medisorbon is a synthetic dealuminized Y-Zeolite that has hydrophobic properties. It can be used at high temperatures and is acid resistanct. This proprietary zeolite captures mercury, dioxins, and furans in flue gas. The zeolite also captures a small amount of the sulfur dioxide (SO_2) emissions. Medisorbon is more expensive than activated carbon; but, it only needs replacement every three years. The operation costs are comparable to activated carbon.(Samdani, 1994) The zeolite is regenerable by decomposing or distilling the adsorbed substances; it can be regenerated several times. The Medisorbon process is almost maintenance free. No corrosion problems occur from the zeolite since the formation of sulfuric acid (H_2SO_4) is low.(Caruana, 1996)

Fly Ash

Highly active sites on the surface of the fly ash particles make it a promising candidate for adsorbing mercury(II) particles. Mercury(II) is reduced to mercury(I) which is reduced to mercury(0) at high temperatures. The most important factors for mercury adsorption on fly ash are adsorption temperature, contact time, specific surface area, and carbon content. If mercury is not in a oxidized form, the adsorption capacity is less. Operation must take place under 100°C for maximum mercury adsorption.(Mojtahedi and Mroueh, 1989)

Fly ash is one of the least expensive adsorbents. It has a smaller surface area than activated carbon and leads to uniform diffusion of the adsorbate. Bonding is induced between the adsorbent and adsorbate due to the surface charge (chemical adsorption).

Calcium Compounds

Calcium compounds used as adsorbents for mercury have the best removal rate using wet-dry methods. Mercury adsorption must be done under low temperatures. In the temperature range of 180-220°C, there is almost no mercury removal. Under 100°C, removal rates range for zero to twenty-five percent.(Mojtahedi and Mroueh, 1989). Removal rates for Hg (II) with calcium hydroxide ($Ca(OH)_2$) are approximately 95 percent at bed temperatures between 75°C and 100°C.(Lancia, *et al.*, 1993) This removes ninety percent of the mercury, mostly $HgCl_2$ and elemental mercury.

Palladium Chloride

Chromasorb W solid particles (mesh 30/60) coated with palladium chloride ($PdCl_2$) can be used as a mercury adsorbent. Mercury emissions of 6-20 mg/m^3 have been reduced to 0.005 mg/m^3. The percentage removal is not changed with the addition of water vapor or sulfur dioxide (SO_2).(Nguhen, 1979)

Manganese Oxide

Alekseevskii, *et al.*, proved that MnO_2 has high adsorptive properties for Hg as a result of the high oxidation power of Mn^{+4}.(Cavallaro, *et al.*, 1982) The study of manganese based reagents supported on an inert medium was performed at atmospheric pressure and ambient temperature. γ-Al_2O_3 has a low mercury sorption capacity. Copper doped γ-Al_2O_3 has higher activity than aluminum oxide alone.

The powerful oxidizing nature of Mn^{+4} has been demonstrated in oxidation reactions of CO, SO_2, and aniline.(Cavallaro, *et al.*, 1982) Oxidation properties of MnO_2 are determined by the presence of oxygen dissociatively chemisorbed on the surface.

Iron Compounds

Iron compounds are readily available at a low cost and have the capacity to adsorb mercury and sulfur. Maximum adsorption of Hg takes place at high temperatures. There is only minimal information on the sorption kinetics and sorption capacity for Hg^0 and cannot be used practically for trace element sorption purposes.(Mojtahedi and Mroueh, 1989)

Sorbalit

Sorbalit controls emissions of acid gases, Hg, and organics in a single application. The sorbalit mixture consists of sulfur, activated carbon, and lime in the form of calcium hydroxide or calcium oxide. The activated carbon adsorbs organic dioxins, lime adsorbs the acidic SO_2, and the sulfur adsorbs the Hg. Sorbalit captured 88 % of the total Hg and 83 % of the vapor phase Hg under normal Hg capture conditions. Sorbalit has also been tested under difficult Hg capture conditions, high temperature and low moisture. Under these conditions, Sorbalit captured 44 to 55 % of the vapor phase Hg.(Licata, *et al.*, 1994)

Noble Metals

Noble metals adsorb mercury by amalgamation. Tin, zinc, copper, lead, cadmium, silver, and copper alloys form mercury amalgams.

Silver/4A molecular sieves remove mercury and moisture from flue gases. It is regenerable and has a long-term stability.(Yan, 1994) Zeolites do not generate mercury adsorbent waste and mercury can be recovered as a product.(Weekman and Yan, 1995)

ADA Technologies, Inc., has developed the Mercu-RE process. This system not only captures the mercury, it recycles it. The mercury removal efficiencies for all mercury forms are claimed to be above ninety percent. Currently, it has been tested for flow rates up to fifty actual cubic feet per minute and temperatures up to 350°F.(Carnana, 1996)

CHAPTER III

EQUIPMENT AND PROCEDURE

This chapter describes the methodologies used to prepare a range of metal oxides and to evaluate the adsorption capacities of these metal oxides and fly ash for mercury.

Equipment Setup

Figure 1 below shows a schematic of the equipment setup.

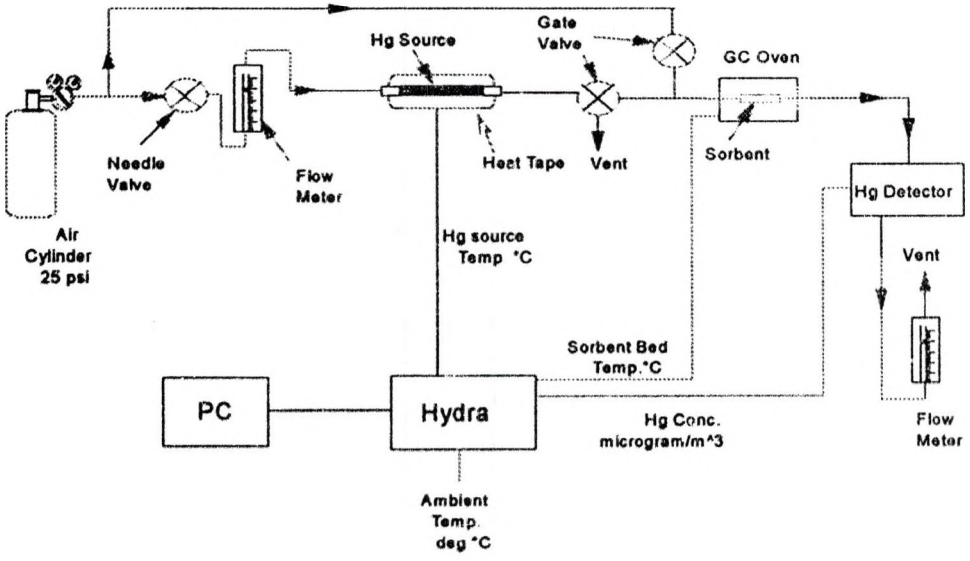

Figure 1: Equipment Schematic

A flow meter controls the flow of air or nitrogen through the mercury source. This flow is approximately 100 cm^3 per minute. Compressed air is used but the nitrogen is bled from a liquid nitrogen tank. The nitrogen contains a negligible amount of oxygen and moisture which will not drastically affect the results of the experimentation.

The diffusion rate of mercury is defined by the temperature of the permeation tube. The tube is calibrated to emit a specific concentration of mercury at a certain temperature. The range of mercury concentrations that can be emitted into the air is 100-500 $\mu g/m^3$. In this study, the source was maintained at 140°C at which it emits 320 $\mu g/m^3$ of mercury with our flow rate.

A gate valve allows the mercury to either be vented and captured or passed through the metal oxide sample in the gas chromatography (GC) oven. The samples prepared as metal oxides are contained in small tubes. The tubes are placed in the GC oven and heated. The mercury laden gas passes through the sample tubes and is adsorbed depending on the oxide. The effluent passes through a continuous mercury vapor monitor that measures the mercury present in the effluent. The efficiency of the metal oxides for elemental mercury adsorption is calculated from the amount of mercury remaining after passing through the oxide bed.

A Hydra Data Logger measures the adsorbent bed temperature, ambient temperature, and the mercury concentration passing through the continuous mercury vapor monitor once every 60 seconds A computer is connected to the Hydra Data Logger storing the data for later reduction.

After the mercury detector, the effluent passes through a second flow meter that measures the flow of air or nitrogen out the vent where any remaining mercury is captured in an iodized carbon filter.

EPM Model 793 Continuous Vapor Monitor

The EPM Mercury Vapor Monitor Model 793 is a direct reading instrument for the continuous determination of mercury vapor concentration in air. It is produced by Environmental & Process Monitoring b.v., Dalerstraat 32, Netherlands, +31 (0) 5916 1828. A discharge type ultraviolet (UV) lamp generates ultraviolet light that is used as the light source. An optical filter selects a narrow spectral band containing the mercury line at 253.4 nanometers (ηm). The measuring beam, part of the light source, passes through a measuring cuvette to a photodiode, while a reference beam passes through the reference cuvette and is detected by a second diode. Both photodiode signals are compared continuously. The liquid crystal display (LCD) reading is linear with the concentration due to the use of a logarithmic amplifier circuit.

The samples were then tested for bonding structure using an Nicolet Magna Fourier Transform Infrared Spectrophotometer. The data was collected at $(8\ cm)^{-1}$ resolution. A Barnes Collector Model #869-032400 Diffuse Reflectance Cell was used with the infrared spectrophotometer.

Preparation of Materials

A majority of the samples were prepared by impregnating an adsorbent matrix with the test metal oxide. The adsorbent matrices used were aluminum oxide (Al_2O_3), carbon, and y-zeolite. Most of the procedures closely resemble the following description for

preparing manganese oxide (MnO_2) on Al_2O_3 formed from manganese nitrate $(Mn(NO_3)_2)\cdot 6H_2O$. Sample calculations are given in Appendix A: Calculations.

Preparation Technique #1 - Utilization of 25 wt % solution

This technique consisted of preparing a 25 wt % solution of the metal oxide precursor which was then combined with the support (Al_2O_3, carbon, zeolite). The 25 wt % solution was prepared and mixed with 10.00 g of Al_2O_3 and dried at 100°C for at least 12 hours. The sample is then oxidized/activated by heating in a furnace in air.(Cavallaro, *et al.*, 1982) Table 1 shows the recipe used to prepare a 4.4 wt % MnO_2 on Al_2O_3 sample.

Table 1: Recipe For 4.4 wt % MnO_2 on Al_2O_3

Step #		Procedure
1	Prepare of $Mn(NO_3)_2\cdot 6H_2O$ Solution	Add 3.33 g $Mn(NO_3)_2\cdot 6H_2O$ to 10.00 g distilled H_2O
2	Prepare 7 wt % MnO_2/Al_2O_3 Sample	Mix 6.19 g of solution with 10.00 g Al_2O_3
3	Dry Sample	Place in drying oven (100°C) overnight
4	Activate Sample	Place in furnace (200°C) and heat for 4 hours

This technique was used for several other samples. Table 2 shows the various samples prepared including the precursor used to prepare the oxide and the activation/oxidation temperature used.

Table 2: Samples Following Sample Preparation Technique #1		
Sample	**Test Oxide Precursor**	**Activation Temperature (°C)**
MnO_2/Al_2O_3 (4.4 wt %)	Manganese Nitrate ($Mn(NO_3)_2*6H_2O$)	200°C 500°C 700°C
MnO_2/carbon (4.1 wt %)	Manganese Nitrate ($Mn(NO_3)_2*6H_2O$)	200°C 400°C
MnO_2/Al_2O_3 (2.8 wt %)	Manganese Acetate ($Mn(C_2H_3O_2)_2*3H_2O$)	200°C 500°C 600°C 700°C
MnO_2/Al_2O_3 (5.3 wt %)	Manganese Acetate ($Mn(C_2H_3O_2)_2*3H_2O$)	200°C 250°C 300°C 350°C 400°C
MnO_2/y-zeolite (2.2 wt %)	Manganese Nitrate ($Mn(NO_3)_2*6H_2O$)	200°C
Fe/Al_2O_3 (4.3 wt %)	Iron Nitrate Method #1 ($Fe(NO_3)_3*9H_2O$)	200°C 400°C 500°C 600°C
Fe/Al_2O_3[1]	Iron II Sulfate ($Fe_2(SO_4)_3*nH_2O$)	200°C 400°C 500°C 600°C 700°C
Fe/Al_2O_3 (4.0 wt %)	Iron III Sulfate ($FeSO_4*7H_2O$)	200°C 400°C 500°C 600°C 700°C
Cr/Al_2O_3 (4.0 wt %)	Chromium Nitrate ($Cr(NO_3)_2*9H_2O$)	200°C
Ni/Al_2O_3 (5.0 wt %)	Nickel Nitrate ($Ni(NO_3)_2*6H_2O$)	200°C
Co/Al_2O_3 (4.8 wt %)	Cobalt Nitrate ($Co(NO_3)_2*6H_2O$)	200°C

[1]Actual weight percent could not be calculated because the weight of hydrate was unknown.

Preparation Technique #2 - Preparation of 7 wt % Samples

Another procedure was used to prepare sodium sulfate (Na_2SO_4) on Al_2O_3. This procedure was based on seven weight percent Na_2SO_4. The recipe for seven weight percent Na_2SO_4 on Al_2O_3 is listed in Table 3.

Table 3: Recipe for 7 wt % Na_2SO_4 on Al_2O_3

Step #		Procedure
1	Dissolve Na_2SO_4 in H_2O	Add 2 ml distilled H_2O to 0.70 g Na_2SO_4
2	Prepare 7 wt % Na_2SO_4/Al_2O_3 Sample	Add solution dropwise to 10.00 g Al_2O_3 with stirring
3	Dry Sample	Place sample in drying oven (100°C) overnight
4	Activate Sample	Place Al_2O_3/Na_2SO_4 sample in furnace (200°C) and heat for 4 hrs

This technique was used for several other samples. Table 4 shows the various samples prepared. The table includes the activation/oxidation temperature used.

Table 4: Samples Following Sample Preparation Technique #2

Sample	Test Oxide Precursor	Activation Temperature (°C)
$MnSO_4/Al_2O_3$ (7 wt %)	$MnSO_4$	200°C 400°C 600°C
Mn/Al_2O_3 (7 wt %)	$KMnO_4$	No Activation 200°C
Fe/Al_2O_3 (7 wt %)	$(CH_3CO_2)_2Fe$	[illegible] 400°C 600°C 700°C
Fe/Al_2O_3 (7 wt %)	$FeCl_3$	200°C
NH_4VO_3/Al_2O_3 (7 wt %)	NH_4VO_3	200°C 400°C
$Ti(OC_3H_7)_4/Al_2O_3$ (7 wt %)	$Ti(OC_3H_7)_4$	200°C 400°C
$Cu(NO_3)_2/Al_2O_3$ (7 wt %)	$Cu(NO_3)_2$	200°C 400°C

Sample Preparation Technique #3

The procedure for preparing 4.4 wt % MnO_2 and 1 wt % $Cu(NO_3)_2$ on Al_2O_3 is listed in Table 5.

Table 5: Recipe for 4.4 wt % MnO_2 and 1 wt % $Cu(NO_3)_2$ on Al_2O_3

Step #		Procedure
1	Prepare solution of $Mn(NO_3)_2 \cdot 6H_2O$	Add 3.33 g of $Mn(NO_3)_2 \cdot 6H_2O$ to 10.00 g distilled H_2O
2	Prepare 7 wt % MnO_2 and 1 wt % $Cu(NO_3)_2$ on Al_2O_3	Mix 6.19 g solution with 10.00 g Al_2O_3 and 0.12 g $Cu(NO_3)_2$
3	Dry Sample	Place sample in oven (100°C) and dry overnight
4	Activate Sample	Place sample in furnace (200°C) for 4 hrs

Several other samples followed the above procedure. Table 6 lists their activation temperatures and precursor for the test compounds.

Table 6: Samples Following Sample Preparation Technique #3

Sample	Prepared From	Activation Temperature (°C)
MnO_2 (4.4 wt %) & H_2SO_4 (1 wt %)/Al_2O_3	$Mn(NO_3)_2$	No Activation
MnO_2 (4.4 wt %) & Na_2SO_4 (1 wt %)/Al_2O_3	$Mn(NO_3)_2$	No Activation
MnO_2 (4.4 wt %) & $MnSO_4$ (1 wt %)/Al_2O_3	$Mn(NO_3)_2$	No Activation
Mn (7 wt %) & Oxalic Acid (10 wt %)/Al_2O_3	$KMnO_4$	No Activation 200°C
Mn (7 wt %) & Hydrogen Peroxide (5 wt %)/Al_2O_3	$KMnO_4$	No Activation 200°C

Recipe for $Fe(NO_3)_3$ Method #2

The second preparation procedure for $Fe(NO_3)_3$ on Al_2O_3 is listed in Table 7.

Table 7: Recipe For $Fe_2(NO_3)_3/Al_2O_3$ Method #2

Step #		Procedure
1	Prepare Al_2O_3 solution	Add 10 g Al_2O_3 to 1000 g H_2O. Stir for 5 mins.
2	Prepare $Fe(NO_3)_3 \cdot 9H_2O$ solution	Add 2 g $Fe(NO_3)_3 \cdot 9H_2O$ to 80 g distilled H_2O. Stir for 5 min.
3	Combine solutions	Combine solutions with stirring.
4		Add 40 g conc. NH_3OH & 400 ml distilled H_2O to solution.
5	Dry solution	Air dry solution in hood for 72 hrs with constant stirring.
6	Activate samples	Divide dry sample by three.
7	Activate samples	Do not activate the 1st sample
8		Place 2nd sample in furnace for 4 hrs at 200°C
9		Place 3rd sample in furnace for 4 hrs at 400°C

Recipe for MnOOH and Mn_2O_3

The recipe for manganese oxyhydroxide (MnOOH) and manganese sesquioxide (Mn_2O_3) is listed in Table 8. The procedure was obtained from the Journal of the American Chemical Society, "Solid Oxides and Hydroxides of Manganese".(Moore, *et al.*, 1950)

Table 8: Recipe for $MnOOH$ and Mn_2O_3		
Step #		**Procedure**
1	Prepare $MnSO_4 \cdot 4H_2O$ solution	Mix 5 ½ g $MnSO_4 \cdot 4H_2O$ with 875 ml distilled H_2O.
2		Add 3 ml 30 wt % H_2O_4.
3		Add 125 ml 0.5 M NH_3OH.
4	Formation of MnOOH (brown precipitate)	Boil solution with constant stirring.
5		Filter & wash solution.
		Air dry ½ of sample.
6	Formation of Mn_2O_3 (black precipitate)	Dry ½ of sample under vacuum at 250°C for 72 hours.

Recipe for Iron Oxides

Feroxyhyte was prepared from $FeCl_2$ and NaOH. Mn-Fe Goethite was prepared from $Fe(NO_3)_3$, $Mn(NO_3)_2$, and sodium hydroxide (NaOH). Geothite was prepared from $Fe(NO_3)_3$ and Potassium Hydroxide (KOH). Lepidocrocite was prepared from $FeCl_2$ and NaOH. Ferrihydrite was prepared from $Fe(NO_3)_3$. 2-Line Ferrihydrite was prepared from $Fe(NO_3)_3$ and KOH. Maghemite was prepared from $FeCl_3$ and $FeCl_2$. Hematite was prepared from $Fe(NO_3)_3$, KOH, and $NaHCO_3$. Magnetite was prepared from $FeSO_4$, KNO_3, and KOH. Various iron oxides whose formulas are given in Table 9 were prepared according to details given in Iron Oxides in the Laboratory. Table 9 also lists the page number for each procedure.(Schwertmann, *et al.*, 1991)

Table 9: Reference Page Numbers For Iron Oxides		
Iron Oxide	**Formula**	**Reference Page Number***
Maghemite	γ-Fe_2O_3	117
Hematite	α-Fe_2O_3	103
Magnetite	Fe_3O_4	111
Feroxyhyte	δ'-FeOOH	85
Lepidocrocite	γ-FeOOH	81
Geothite	α-FeOOH	64
Mn-Fe Geothite	$(Fe_{1-x}Mn_x)OOH$	73
Ferrihydrite	$Fe_5HO_8*4H_2O$	89
2-Line Ferrihydrite	$Fe_5HO_8*4H_2O$	90

*in "Iron Oxides in the Laboratory"(Schwertmann, *et al.*, 1991)

Description of Ash Samples

Table 10 gives a description of each of the ashes tested.

Infrared Spectoscopy of Samples

The procedure for preparing samples for infrared spectoscopy is listed below. 400 mg of KBr was mixed with the sample. The amount of sample used depended on if it was coated on a support. 25 mg was used if the sample was not on support and 100g if it was on a support. The spectra was obtained at single beam mode where the KBr background was subtracted. The support was not subtracted from the IR spectra.

Table 10: Description of Ashes			
Ash	**METC Code**	**Coal Utilization Process**	**Fuel**
Bitumin Orimulsion Ash (1.3% Ni & 7.7% Fe_2O_3)	NA	Not Available	Orimulsion
Red Brown Bottom Ash (3.7% Fe_2O_3)	702A	Coal Combustion With Flue Gas Cleaning	Utah subbituminous coal
Grey-Black Bottom Ash (21.2% Fe_2O_3)	502A	Coal Combustion With Flue Gas Cleaning	Illinois #6 bituminous coal
Tan Coal Gasification Ash (11% Fe_2O_3)	302A	Fixed-Bed Coal Gasification	Eastern Kentucky low-sulfur (<1%) bituminous coal
Grey-Black Coal Gasification Ash (23.5% Fe_2O_3)	203	Ash Agglomerating Fluidized-Bed Coal Gasification	Dolomite
Black-Brown Bottom Ash (8.3% Fe_2O_3)	602A	Coal Combustion With Flue Gas Cleaning	North Dakota lignite
Black Gasifier Ash (16.2% Fe_2O_3)	2201A	Fluidized-bed Coal Gasification	Pittsburgh #8 bituminous coal
Grey Economizer Ash (6.2% Fe_2O_3)	2403A	Fluidized-bed Coal Gasification	Illinois bituminous coal
Grey Baghouse Fly Ash (11.8% Fe_2O_3)	2404	Fluidized-bed Coal Gasification	Illinois bituminous coal
Red-Brown Spent Bed Material (25.5% Fe_2O_3)	1202A	Fluidized-bed Coal Gasification	Mixture of Illinois #5 and Illinois #6 coals
Red-Brown Spent Bed Material (21.1% Fe_2O_3)	1204	Fluidized-bed Coal Gasification	Mixture of Illinois #5 and Illinois #6 coals
Grey Fly Ash (12.2% Fe_2O_3)	403A	Coal Combustion With Flue Gas Cleaning	Pittsburgh #8 bituminous coal
Spent Scrubber Sludge (9.1% Fe_2O_3)	503	Coal Combustion With Flue Gas Cleaning	Illinois #6 bituminous coal

* in "Geotechnical/Geochemical Characterization Of Advanced Coal Process Waste Streams: Task 2 Report" (Moretti and Olson, 1992)

Procedure For Experimentation

20-60 mesh aluminum oxide, carbon, and y-zeolite were used as supports. The aluminum oxide and y-zeolite were purchased from Aldrich. The surface areas of these supports were 146.25 m^2/g and 440 m^2/g for Al_2O_3 and carbon. The surface of y-zeolite was not available. These supports were then coated with 4-7 % of various metal oxides. 0.20 g of samples were placed in a 6" long circular glass reactor tube with an outer diameter of 0.20".

Several metal oxides were screened by varying: temperature, presence and amount of oxygen, amount of acid, and the uptake of nitrogen oxide (NO) which is a flue gas component.

Activation energy and the order of reaction was determined by varying the temperature at which adsorption takes place. The initial temperature was 150°C. If the metal oxide did not adsorb the mercury, the temperature was increased to determine if adsorption would occur at a higher temperature.

The experimentation began with simple metal oxides and proceeded to more complex transition or lanthanide metal oxides. The work plan began with manganese oxides coated on aluminum oxide, carbon, and y-zeolite. In the next phase, iron oxides coated on aluminum oxide were tested. Thirdly, iron oxides were tested. Transition metals on aluminum oxide were then tested. Finally, fly ash samples were tested.

CHAPTER IV

RESULTS AND DISCUSSION

The results and discussion will be discussed in this order: supports, manganese oxides on support, iron oxides, iron oxides on aluminum oxide, transition metals on aluminum oxide, and fly ashes. Lastly, overall results will include replication of runs, determination of reaction mechanism, and in-situ activation.

Supports

The supporting matrices used in testing metal oxides were aluminum oxide, carbon, and y-zeolite. These supports were tested for their Hg adsorption capacities. From Table 11, it can be seen that the supports were ineffective for Hg sorption. Due to its larger surface area, carbon adsorbed more Hg than Al_2O_3.

Table 11: Hg Sorption Capacities of Supporting Matrices

Support	% Hg Passed into Effluent at 4 hrs and a Reactor Oven Temp of 150°C
Al_2O_3	84
Carbon	75

Manganese Oxides on Support

Supporting matrices were coated with 4-7 wt % metal oxides to determine if chemical activation increased their Hg adsorption capacities. From the literature review (Chapter II), we know that chemical activation should increase adsorption capacity. Table

12 lists the samples, activation temperatures, reactor oven temperatures, and percentage Hg passed into effluent at a time of 4 hours. Samples that passed less than 10 % Hg were considered effective adsorbents for Hg.

Table 12: Manganese Oxides on Supports

Sample	Activation Temperature (°C)	Reactor Oven Temperature (°C)	% Hg Passed Into Effluent at 4 hrs
MnO_2/Al_2O_3	200	150	0
	500	150	0
	700	150	0
MnO_2/Al_2O_3 & $Cu(NO_3)_2$	200	150	0
MnO_2/y-zeolite	200	150	0
MnO_2/carbon	200	150	26
	400	150	12
Na_2SO_4/Al_2O_3	200	150	100
	400	150	85
	600	150	83
$MnSO_4/Al_2O_3$	200	150	92
	400	150	80
	600	150	78
MnO_2/Al_2O_3 & Na_2SO_4	No Activation	150	0
MnO_2/Al_2O_3 & $MnSO_4$	No Activation	150	0
MnO_2/Al_2O_3 & H_2SO_4	No Activation	150	0
$Mn(C_2H_3O_2)_2/Al_2O_3$ (2.8 wt %)	No Activation	150	65
	200	150	70
	500	150	48
	600	150	46
	700	150	44
$Mn(C_2H_3O_2)_2/Al_2O_3$ (5.3 wt %)	200	150	80
	250	150	0
	300	150	0
	350	150	1
	400	150	0
$KMnO_4/Al_2O_3$	No Activation	150	7
	200	150	0
$KMnO_4/Al_2O_3$ & Oxalic Acid	No Activation	150	0
	200	150	0
$KMnO_4/Al_2O_3$ & Hydrogen Peroxide	No Activation	150	0
	200	150	0
MnOOH	No Activation	150	0
Mn_2O_3	No Activation	150	0
HTO_x	No Activation	150	64

Comparison to Cavallaro, *et al.*

The ambient temperature studies of Cavallaro, *et al.*(1982) provided a baseline comparison for this work. They found that Al_2O_3 did not adsorb mercury. Additionally, MnO_2 on Al_2O_3 was a poor adsorber of Hg, but improved when impregnated on $Cu(NO_3)_2$. Finally, $KMnO_4/Al_2O_3$ was shown to be a good adsorbent for Hg. However, the Cavallaro study is of limited relevance to the adsorption of Hg from stack gases because of the associated high temperature. To better simulate stack conditions, the tests in this study were performed at 150°C. The general trends observed at 150°C followed those present at ambient temperature, but MnO_2/Al_2O_3 adsorbed Hg well at 150°C.

Comparison of Supports

Al_2O_3 and carbon supports were tested with and without chemical activation. The supports were coated with MnO_2. Al_2O_3 completely adsorbed Hg with chemical activation; carbon did not (32 % Hg released into the effluent stream). Chemical activation of Al_2O_3 and carbon with MnO_2 is required for significant adsorption of Hg. A probable reaction mechanism for MnO_2 reacting with Hg may be:

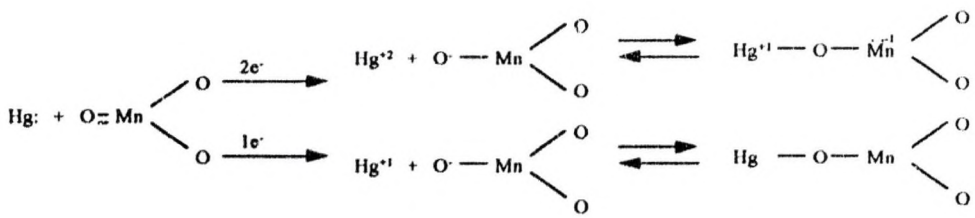

Additionally, Y-zeolite was coated with MnO_2. Figure 2: Comparison of Supports Coated with MnO_2 shows that Al_2O_3 and y-zeolite provided more effective Hg sorption

Rachel Wilkes.

than carbon at an reactor oven temperature of 150°C and time of 4 hours. Carbon has a larger surface area than Al_2O_3 possibly providing more MnO_2 sites for the Hg to react with, increasing the Hg sorption capacity. The results contradict this statement. One possible explanation is that MnO_2 has a stronger interaction with carbon than the Al_2O_3 or y-zeolite, making MnO_2 less available for bonding with Hg^0.

Figure 2
Comparison of Supports With MnO2

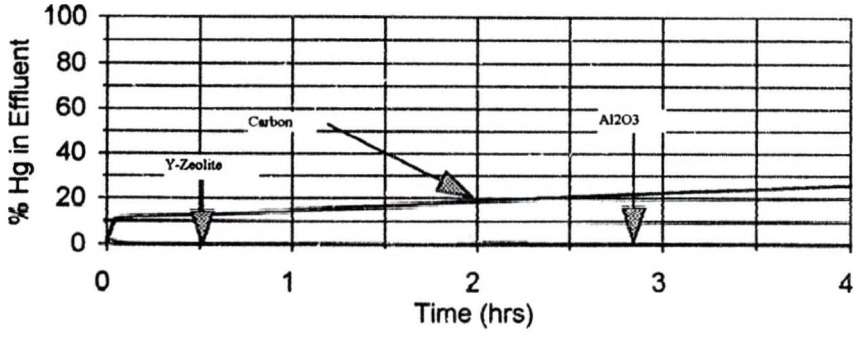

Comparison of Sulfates on Al_2O_3 with and without MnO_2

$MnSO_4/Al_2O_3$ and Na_2SO_4/Al_2O_3 activated at 200°C, 400°C, and 600°C were not effective adsorbents for Hg. None of the samples adsorbed more than 23 % of the mercury passed from the source. IR Spectroscopy showed that $MnSO_4$ did not decompose to MnO_2 at any activation temperature. The results from performing IR spectroscopy on manganese oxide samples is included in Appendix C given in Table 23: Infrared Spectroscopy Results. It may possible that $MnSO_4/Al_2O_3$ was not activated at a

high enough temperature so that decomposition to MnO_2/Al_2O_3 could take place. This could further apply to Na_2SO_4/Al_2O_3.

It was of interest to the determine the effect of the addition of sulfate to MnO_2/Al_2O_3 since flue gas contains SO_2 and in the presence of oxygen it can oxidize to SO_4^{-2}. MnO_2/Al_2O_3 coated with $MnSO_4$, Na_2SO_4, and H_2SO_4 adsorbed all the Hg passed into the effluent. Therefore, there is no sulfate interference, inhibition, or poisoning. IR spectra show that H_2SO_4 did not convert MnO_2 on Al_2O_3 to a different compound with its addition to the sample. Manganese oxide impregnated on alumina would be an effective adsorbent for Hg when used in streams contain SO_2.

Comparison of Al_2O_3 coated with 2.8 and 5.3 wt % $Mn(C_2H_3O_2)_2$

$Mn(C_2H_3O_2)_2/Al_2O_3$ was prepared coating 2.8 and 5.3 wt % metal oxide onto the Al_2O_3. Adsorption Efficiencies in Table 12 show that the 2.8 wt % sample was ineffective for Hg sorption at a reactor oven temperature of 150°C. However 5.3 wt % $Mn(C_2H_3O_2)_2/Al_2O_3$ activated at 250°C was effective for Hg removal at an oven temperature of 150°C. Therefore, this sample required a minimum activation temperature (250°C) to become a good adsorbent for Hg. The activation temperature must be high enough to decompose the manganese acetate and convert it to the oxide. This was evident in the IR spectra results; there were no acetate peaks for $Mn(C_2H_3O_2)_2/Al_2O_3$ activated at 250°C. The higher weight percent $Mn(C_2H_3O_2)_2/Al_2O_3$ is a better adsorbent because it includes more active sites for Hg adsorption.

Chemical Impregnation of Carbon

Carbon was tested alone and with chemical impregnation of $Mn(NO_3)_2$. $Mn(NO_3)_2$/carbon was activated at 200°C and 400°C. This was done to determine if $Mn(NO_3)_2$/carbon would become activated/oxidized (forming MnO_2/carbon) at a certain temperature. Table 12 shows that MnO_2/carbon had an increase in adsorption capacity with activation at a higher temperature; although it did not completely adsorb all the Hg.

Figure 3: Carbon Adsorption Efficiencies demonstrates that the carbon has some sorption capacity, since the bed initially removes some mercury. However, the sorption capacity of the non-treated carbon is quickly overwhelmed. The chemically treated carbons demonstrated improved mercury sorption. The higher activation temperature resulted in an adsorbent with better sorption capacity. This is probably due to a greater decomposition of $Mn(NO_3)_2$ of MnO_2 at the higher temperature (400°C) resulting in larger number of active sites.

Figure 3
Carbon Adsorption Efficiencies

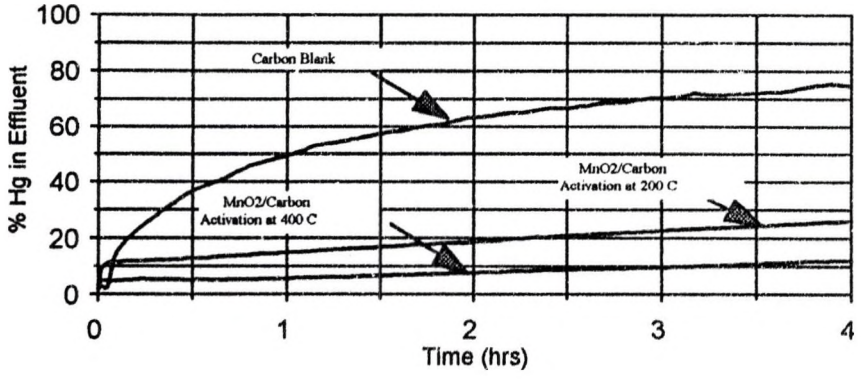

Iron Oxides

Table 14 lists the results of testing iron oxides for their effectiveness as mercury adsorbents. The table includes the % Hg passed into the effluent at 30 minutes for each reactor oven temperature used in testing. Figure 4 is a representative graph of the results from testing iron oxides different oven temperatures. It shows that maghemite was an effective adsorbent for Hg at a reactor oven temperature of 200°C.

Table 13: Iron Oxides

Sample	Reactor Oven Temperature (°C)	% Hg Passed Into Effluent
Maghemite	100	78
	150	12
	200	1, 2
	233	0
	266	0
	300	0
	333	4
	366	11
	400	3
Hematite	60	81
	80	81
	100	78
	120	78
	140	80
	150	82
	160	79
	180	83
	200	84
	250	57
	300	80
	350	78
	400	72
Magnetite	60	100
	80	100
	100	100
	120	98
	140	100
	160	99
	180	100
	200	98
	250	86
	300	47
	350	38
	400	18

Table 13 cont.

Feroxyhyte	60	94
	80	93
	100	92
	120	96
	140	96
	160	95
	180	83
	200	0
Lepidocrocite	60	96
	80	92
	100	91
	120	94
	140	93
	160	92
	180	74
	200	5
Goethite	60	76
	80	55
	100	53
	120	39
	140	45
	160	35
	180	4
	200	0
Mn-Fe Goethite	60	95
	80	95
	100	96
	120	95
	140	96
	160	91
	180	95
	200	89
Ferrihydrite	60	83
	80	92
	100	97
	120	100
	140	100
	160	95
	180	71
	200	99
2-Line Ferrihydrite	60	91
	80	89
	100	82
	120	81
	140	35
	160	17
	180	0
	200	0

Determination of Activation Temperature

Several iron oxides (maghemite, feroxyhyte, lepidocrocite, goethite, and 2-line ferrihydrite) were effective at 200°C and it had to be determined if they were reaching an

activation (oxidation) temperature. After testing the iron oxide at 200°C, the reactor oven temperature was then decreased to 150°C to determine if the sample was still effective for Hg adsorption. Table 14 shows the results of testing several samples for their activation temperature. These results can be visually seen in Figures 5 (maghemite), 6 (feroxyhyte), 7 (lepidocrocite), 8 (goethite), and 9 (2-line ferrihydrite).

Table 14: Activation Temperature Determination For Iron Oxides

	% Hg Passed into Effluent at 30 min	
	Oven Temp 200°C	**Oven Temp 150°C**
Maghemite	5	98
Feroxyhyte	0	4
Lepidocrocite	5	96
Goethite	0	79
2-Line Ferrihydrite	0	26

Maghemite, lepidocrocite, goethite, and 2- line ferrihydrite passed the same amount of Hg into the effluent at an reactor oven temperature of 150°C before and after testing at 200°C. IR spectra showed that maghemite, goethite, and 2-line ferrihydrite did not form different compounds at 200°C. Therefore, they must be used at a temperature of 200°C to be effective adsorbents (operating under chemisorption). From IR spectra, it was determined that lepidocrocite formed maghemite at 200°C. Maghemite requires a higher oven temperature to be an effective adsorbent, hence, the lepidocrocite sample should also. Feroxyhyte was an effective adsorbent for Hg when reactor oven temperature was decreased to 150°C. IR spectra showed that feroxyhyte formed new bonds at 200°C. The product must be an active iron oxide.

Determination of activation temperature was also made by heating the iron oxides in a furnace to determine if they became activated/oxidized at those temperatures. Table 15 lists the % Hg passed into the effluent for samples heated at several temperatures. Hematite's adsorption capacity did not change with activation at a higher temperature. Mn-Fe goethite's adsorption capacity increased at higher temperatures; although, activation at 400°C was significantly better than at 500°C. The two explanations for this are that scatter in the experimental data makes the values indistinguishable or that something more significant is happening at 400°C that is beyond the scope of this study.

Table 15: Iron Oxide Adsorption Capacity Determination At Various Activation Temperatures

Iron Oxide	Activation Temperature (°C)	% Hg Passed into Effluent at Reactor Oven Temp of 150°C and 4 hrs
Hematite	No Activation	82
	250	78
	400	82
Mn-Fe Goethite	No Activation	93
	400	52
	500	77

Structure of Iron Oxides

The active iron oxides all were less dense than the inactive iron oxides and their structure includes vacancies.(Schwertmann, *et. al.*, 1991) There is a correlation between the density of iron oxides and their adsorption efficiencies. These iron oxides were formed with different configurations of iron and oxygen in tetrahedra and octahedra. The structure of the individual oxides will be discussed in Table 16. (Schwertmann, *et. al.*, 1991)

Table 16: Structure of Iron Oxides	
Iron Oxide	**Structure**
Maghemite	One half of the interstices are tetrahedrally coordinated with oxygen and 2/3 are octahedrally coordinated. Five sixths of total available positions are filled by Fe^{3+}; the rest are vacant. Maghemite has different symmetries depending on the degree of ordering of the vacancies.
Feroxyhyte	Feroxyhyte has a hematite-like structure which is hexagonally close-packed oxygen planes with Fe ions in octahedral interstices. But, feroxyhyte's structure includes vacant Fe sites.
Lepidocrocite	Lepidocrocite is composed of double bands of octahedra which share edges to form zig-zag layers which are connected to each other by hydrogen bonds. Only half of the octahedral interstices are filled with Fe^{3+}.
Goethite	Geothite is composed of double bands linked by corner-sharing in such a way as to form 2 x 1 octahedra "tunnels" crossed by hydrogen bridges. Only half of octahedral interstices are filled with Fe^{3+}.
Magnetite	One half of the interstices in magnetite are tetrahedrally coordinated with oxygen and 2/3 are octahedrally coordinated. All positions are filled with Fe, tetrahedral positions filled with Fe^{3+} and the octahedral ones by equal amounts of Fe^{3+} and Fe^{2+}.
Hematite	Hematite is composed of layers of FeO_6 in octahedra which are connected by edge-and face-sharing. Two thirds of the octahedral interstices are filled with Fe^{3+}. Face sharing is accomplished by a slight distortion of the octahedra which causes a regular displacement of the Fe ions. The distortion and absence of H bonds yield a compact structure which is responsible for the high density.
Mn-Fe Goethite	Contains Mn(III) and Fe(III) with a crystal structure similar to goethite; except, two of the unit cell edge lengths are shorter and one is longer.
Ferrihydrite	Ferrihydrite has a hematite-like structure composed of hexagonally close-packed oxygen planes with Fe ions in octrahedral interstices. Its structure includes vacancies.
2-Line Ferrihydite	Structure similar to ferrihydrite except that it has a different structural order and crystaline plane.

Magnetite, hematite, Mn-Fe goethite, and ferrihydrite's structures do not include vacancies which increases their densities. It is therefore harder for the Hg^0 to be oxidized by the molecules on the inside or edges of the structure. IR spectra showed that the hematite structure remained the same with heating. Therefore, hematite would remain inactive at this temperature; as evident from the adsorption results. IR spectra showed that magnetite formed hematite at 200°C, which was shown to be inactive for Hg

adsorption. At a reactor oven temperature of 150°C, Mn-Fe goethite was shown to contain goethite which was inactive at this temperature. IR spectra indicated that a greater amount of another compound was present at 200°C; hence, this may explain why it was not a good adsorbent at 200°C. Goethite was an effective adsorbent for Hg at 200°C. Another possible explanation for Mn-Fe goethite inactivity may be that manganese and/or iron were not in their highest oxidation state. Ferrihydrite's structure includes vacancies; but, adsorption results show that it is an ineffective adsorbent for Hg. A probable explanation is its hematite-like structure; hematite was previously found to be inactive.

Iron Oxides on Aluminum Oxide

Several iron oxides were tested for their Hg adsorption capacity. Table 17 shows % Hg passed into the effluent for several iron oxides on aluminum oxide activated at various temperatures.

Iron III Sulfate under heat should decompose to form a oxide. IR spectra showed that sulfate was present in samples activated at 200°C and 400°C. Hence, the sample did not decompose at these activation/oxidation temperatures. Figure 10 shows the inactivity of Fe_2SO_4/Al_2O_3 activated at 200°C, 400°C, and 700°C.

Iron II Sulfate forms a hydroxy oxide which always forms maghemite with activation. Iron II Sulfate was a good adsorbent when activated at 200°C indicating that at this activation temperature iron II sulfate is decomposing to iron oxide. At an activation temperature of 400°C, it lost its sorption capacity. This loss maybe explained

Table 17: Iron Oxides on Aluminum Oxide		
Sample	**Activation Temperature (°C)**	**% Hg Passed into the Effluent at Reactor Oven Temp of 150°C and 4 hrs**
$Fe_2(SO_4)_3/Al_2O_3$	200	64
	400	78
	500	82
	600	84
	700	77
$FeSO_4/Al_2O_3$	200	8
	400	78
	500	89
	600	71
	700	81
$(CH_2CO_2)_2Fe/Al_2O_3$	200	70
	400	83
	500	84
	600	60
	700	78
$FeCl_3/Al_2O_3$	200	0
Fe_2O_3/Al_2O_3[1]	200	78
	400	87
	500	69
	600	91
$FeOOH/Al_2O_3$[2]	No Activation	26
	200	0
	400	85

[1] $Fe(NO_3)_3/Al_2O_3$ Preparation Method #1
[2] $Fe(NO_3)_3/Al_2O_3$ Preparation Method #2

by the formation of the inactive hematite. IR spectra of $FeSO_4/Al_2O_3$ activated at 200°C and 400°C did not show a peak corresponding to sulfate. A sharp peak was in the spectra for activation at 200°C which does not correspond to any of the iron oxides already studied. This peak disappeared in the sample activated at 400°C. The functional group

corresponding to this peak probably was causing the activity of the sample. Figure 11 shows that $FeSO_4/Al_2O_3$ became inactive at an activation temperature above 200°C.

Upon heating, iron acetate should decompose to form an iron oxide. IR spectra showed that the acetate in the sample activated at 200°C did not decompose, although some decomposition did occur at 400°C. This was indicated by a smaller IR peak. IR spectra previously showed that manganese acetate decomposed at 400°C but not at 200°C. Figure 12 shows that the adsorption efficiency of $(CH_2CO_2)_2Fe/Al_2O_3$ did not increase with activation at a higher temperature.

Iron nitrate was impregnated into alumnia by two methods. The first sorbent was prepared from the acid form. Iron III in that case always forms hematite, which is known to be inactive and will not adsorb Hg. The second sorbent was prepared from a hydroxy oxide which is known to be active and will adsorb Hg.

IR spectra showed that the structure of the two samples were completely different. Both samples did contain nitrate which had not decomposed to an oxide. Figure 13 shows that Fe_2O_3/Al_2O_3 was an ineffective adsorbent for Hg at several activation temperatures. The second sample did show an IR peak corresponding to the hydroxy oxide. Figure 14 shows that $FeOOH/Al_2O_3$ was an effective adsorbent for Hg when activated at 200°C but became uneffective with activation at a higher temperature.

Chlorides have a high adsorption capacity for Hg at the temperatures studied. Iron chloride activated at 200°C exhibited good adsorption capacity at a reactor temperature of 150°C.

Transition Metals

This section lists the results obtained in the testing of transition metal oxides on aluminum oxide to determine if they were good adsorbents for mercury. Table 18 lists the sample tested with its activation temperature and mercury adsorption capacity.

Table 18: Transition Metal Adsorption Capacities

Sample	Activation Temperature (°C)	% Hg in Effluent at 4 hrs and Reactor Oven Temp of 150°C
$Cr(NO_3)_2/Al_2O_3$	200°C	2
$Ti(OC_3H_7)_4/Al_2O_3$	200°C	79
	400°C	86
$Ni(NO_3)_2/Al_2O_3$	200°C	1
$Cu(NO_3)_2/Al_2O_3$	200°C	77
	400°C	81
$Co(NO_3)_2/Al_2O_3$	200°C	48
	400°C	77
	500°C	99
NH_4VO_3/Al_2O_3	200°C	63
	400°C	85
NH_4VO_3/Gascoyne Lignite	400°C	70

$Cr(NO_3)_2/Al_2O_3$ and $Ni(NO_3)_2/Al_2O_3$ were proven effective adsorbents for Hg. The other samples failed as adsorbents for Hg. This nickel result is especially important because of its presence in bituminous orimulsion ash. The inactivity of titanium isopropoxide is due to its decomposition to form titanium oxide which is not a good oxidizing agent for most compounds. Copper nitrate was not a good adsorbent for Hg. It

is known that copper chloride is a good adsorbent for Hg. More studies should be done to determine if the copper ion is active component for adsorbing Hg.

Ammonium vanadate is known oxidize some compounds. It decomposes to form vanadium oxide (V_2O_5). Vanadium oxide was not a good adsorbent for Hg when coated on aluminum oxide or carbon.

$Ti(OC_3H_7)_4/Al_2O_3$, $Cu(NO_3)_2/Al_2O_3$, $Co(NO_3)_2/Al_2O_3$, and NH_4VO_3/Al_2O_3 showed decreased adsorption capacity with activation at higher temperatures. These samples may be adsorbing at low temperatures under the physisorption principle.

Ashes

This section lists the results obtained in the testing of ashes to determine if they were good adsorbents for mercury. Table 19 lists the ash, US Department of Energy Morgantown Energy Technology Center Code and percentage Hg emitted in effluent at a reactor temperature of 150°C.

The only fly ash found to be a good sorbent for Hg was Bitumin Orimulsion Ash. It has a high nickel (1 percent) and vanadium (12 percent) content. Previous work showed that nickel oxide was an effective adsorbent and that vanadium oxide failed as an adsorbent for Hg. The other adsorbents did not adsorb a majority of the mercury emitted.

There is no relationship between Hg emissions and the type of ash produced in power plants. Iron content does vary with the parent coal, but the major form is hematite. The different types of iron most likely convert to hematite at higher temperatures, and hematite was shown to be inactive. The activity of bitumin orimulsion ash may be due to its high nickel content.

Table 19: Ash Results		
Ash	**METC Code**	**% Hg Emitted**
Bitumin Orimulsion Ash	NA	2
Red Brown Bottom Ash (3.7% Fe_2O_3)	702A	100
Grey-Black Bottom Ash (21.2% Fe_2O_3)	502A	99
Tan Coal Gasification Ash (11% Fe_2O_3)	302A	99
Grey-Black Coal Gasification Ash (23.5% Fe_2O_3)	230	100
Black-Brown Bottom Ash (8.3% Fe_2O_3)	602A	100
Black Gasifier Ash (16.2% Fe_2O_3)	2201A	90
Grey Economizer Ash (6.2% Fe_2O_3)	2403A	94
Grey Baghouse Fly Ash (11.8% Fe_2O_3)	2404	75
Red-Brown Spent Bed Material (25.5% Fe_2O_3)	1202A	86
Red-Brown Spend Bed Material (21.1% Fe_2O_3)	1204	65
Grey Fly Ash (12.2% Fe_2O_3)	403A	95
Spent Scrubber Sludge (9.1% Fe_2O_3)	503	93

Overall Results

The following discussion covers the results from the testing of manganese oxides on supports, iron oxides, iron oxides on aluminum oxide, and transtion metal oxides on aluminum oxide.

Replication of Results

Table 22 presents the results obtained in replicating tests to determine the accuracy of results obtained from the mercury vapor monitor. It can be seen that the actual percentage Hg passed into the effluent varied up to 8 % when replicated. Due to the small

number of runs replicated, this may not be a true indication of the error in calculating percentage Hg passed into the effluent.

Table 20: Replication of Runs		
Sample (Activation at 200°C)	**% Hg Passed Into Effluent**	**Average % Hg Passed Into Effluent**
Na_2SO_4/Al_2O_3	319, 319	319±0
$FeSO_4/Al_2O_3$	9, 8	8.5±0.5
$Mn(C_2H_3O_2)_2/Al_2O_3$	74, 80	77±3
Hematite	84, 83	83.5±0.5
Magnetite	98, 90	94±4

Determination of Reaction Mechanism

Table 20 presents the results obtained from determining the role of oxygen in the sorption of mercury on metal oxides was evaluated. Without oxygen, the reaction is not necessarily catalytic. Iron oxides tested under air and nitrogen gave the same results. Since under both conditions all the mercury passed from the source was adsorbed, molecular oxygen has no effect on the rate of Hg sorption by and therefore is not involved in the reaction. The metal oxide is all that is required for mercury sorption. The metal oxide is therefore oxidizing the mercury and the oxidation state of the metal (e.q. Mn, Fe, Ni) is lowered.

The percentage Hg passed into the effluent increased slightly for maghemite when tested under nitrogen. It is possible that this value is not real, since errors of up to 8 actual %was obtained in replication. If the values are real, there is small catalytic effect of oxygen.

Table 21: Comparison of Adsorption Capacities Using Air and Nitrogen			
		% Hg Passed into Effluent	
Metal Oxide	Activation Temperature (°C)	Air	Nitrogen
MnO_2/Al_2O_3	150	0	0
Maghemite	200	1	7
$FeOOH/Al_2O_3$	200	0	0
$FeCl_3/Al_2O_3$	200	0	0
$Ni(NO_3)_2/Al_2O_3$	200	1	1

In-Situ Activation

Temperature studies were performed on several samples activated at 200°C. They involved testing the same metal oxide with isothermal reaction periods of 30 minutes and then increasing the oven temperature in at approximately 40°C intervals from ambient temperature (25°C) to 350°C and then decreasing the temperature by the same increments. Table 21 shows the oven temperatures, and % Hg passed into the effluent for MnO_2/Al_2O_3 and $Mn(C_2H_3O_2)_2/Al_2O_3$ (2.8 wt %).

Temperature studies were performed on MnO_2/Al_2O_3 and $Mn(C_2H_3O_2)_2/Al_2O_3$ (2.8 wt %). Table 13 shows that MnO_2/Al_2O_3 was effective as an adsorbent for Hg at all reactor oven temperatures. This was not the case for $Mn(C_2H_3O_2)_2/Al_2O_3$ which was ineffective as an adsorbent for Hg below a reactor oven temperature of 220°C. Its effectiveness decreased when the temperature decreased to 100°C. If the reaction is physisorption, the adsorption capacity should decrease with higher activation temperatures. This is not true and there may be an indication of chemisorption.

Table 22: In-Situ Activation of Hg on $Mn(C_2H_3O_2)_2/Al_2O_3$		
Oven Temperature (°C)	**% Hg Passed in Effluent for MnO_2/Al_2O_3**	**% Hg Passed in Effluent for $Mn(C_2H_3O_2)_2/Al_2O_3$ (2.8 wt %)**
20	1	84
60	0	82
100	1	77
140	1	66
180	0	49
220	0	0
260	0	0
300	0	0
330	0	0
350	0	0
330	0	0
300	0	0
260	0	1
220	0	1
180	0	2
140	0	6
100	1	32
60	1	91
20	1	100

These results are presented in Figure 15: In-Situ Activation included in Appendix C.

CHAPTER V

CONCLUSIONS AND RECOMMENDATIONS

Conclusions

This project was initiated to study the mercury sorption properties of metal oxides so that some of sorption processes in fly ash may be understood. The objective of the project was to investigate the fundamental aspects of toxic metal (mercury) sorption by metal oxides. The overall goal of this research is to evaluate the potential for the adsorption of elemental mercury vapor on inorganic oxide materials, determine which metal inorganic oxides can catalyze the oxidation of elemental mercury, and ascertain the nature of the sorption process by examing temperature effects and oxygen requirements.

1. Oxygen is not required for the sorption of mercury on metal oxides. Therefore, the reaction of metal oxides with mercury is not catalytic, but direct oxidation.
2. Chemical impregnation with $Mn(NO_3)_2$, $Mn(C_2H_3O_2)_2$, $KMnO_4$, MnOOH, Mn_2O_3, FeOOH, $FeCl_3$, $Cr(NO_3)_2$, or $Ni(NO_3)_2$ increases the adsorption capacity of aluminum oxide.
3. The addition of sulfate on an active sorbent (e.g. manganese oxide on aluminum oxide) does not poison the sorbent towards mercury adsorption.
4. There is a correlation between the density of iron oxides and their adsorption efficiencies. The lower the density, the higher the adsorption capacity.

5. Fly ashes do not have a high adsorption capacity for mercury due to their conversion of iron compounds to hematite at high temperatures.

Recommendations

Recommendations for further study on this project are listed below.

1. More testing should be done to determine if oxygen is a factor in the adsorption of mercury on metal oxides. Maghemite tested with air and nitrogen showed a slight difference in adsorption efficiencies at an oven temperature of 200°C. It should be determined if this difference is real or due to the error in the mercury measurements.
2. The effect of water vapor in the flue gas should be tested. Inorganic adsorbents are polar and preferentially adsorb water vapor over mercury from the flue gas stream. Water vapor is present in most flue gas streams. It may be found that samples that were previously good adsorbents for mercury may now be poor adsorbents.
3. The adsorption capacity for mercury increased when adding a higher weight percent manganese acetate to aluminum oxide. The exten of addition of manganese acetate before the mercury capacity of the oxde plateaus should be investigated.
4. More testing should be performed to determine the effects of nitrates. Nitrate in the samples prepared did not completely decompose. This important because nitrate decomposition may lead to NO formation thus increasing the leval of No_x in the flue gas.

5. Alternative methods for making goethite should be found and used due to the impurities found the IR spectra. It may be possible to use $FeSO_4$ instead of $FeCl_2$. A critical part of making goethite is the pH; hence, maintenance of the pH is required.

6. The IR spectra of the supports were not subtracted from the total IR spectra. Better interpretation of results may be formed by performing this subtraction. Y-zeolite shows several peaks on the IR spectra and it was difficult to interpret the results of MnO_2 coated on y-zeolite. The peaks for $KMnO_4$, $KMnO_4$ and oxalic acid, and $KMnO_4$ and hydrogen peroxide were indistinguishable due to the large peak for aluminum oxide.

7. A better effort should be made to remove the water vapor from the IR spectrophotometer before testing. Water vapor cause several small peaks to form in the spectra, consequently increasing the difficulty to interpret the results.

8. Infrared spectrophotometry of the fly ash samples should be undertaken to determine if the iron contained in them did form hematite at combustion temperatures.

9. Testing should be performed to determine the oxidation state of each compound. The Mossbauer technique could be used for this. Higher oxidation states usually have better adsorption capacities.

10. X-ray chromatography should be used to determine the crystalline structures of the compounds. It could then be determined if their is a correlation between density and adsorption capacity for all metal oxides.

11. The density of manganese, iron, and transition metal oxides on supports should be compared with adsorption capacities.

APPENDICES

APPENDIX A

CALCULATIONS

Calculations To Determine the Amount For MnO_2 on Al_2O_3

Calculations were made to determine the actual recipe for seven weight percent MnO_2 on Al_2O_3. To make the calculations simple, ten grams of H_2O were used to prepare the $Mn(NO_3)_2$ solution. For convenience, a twenty-five percent $Mn(NO_3)_2$ solution was utilized. Therefore, the amount of $Mn(NO_3)_2 \cdot 6H_2O$ required in the solution is calculated as follows.

X = grams of $Mn(NO_3)_2 \cdot 6H_2O$ required

$$\frac{X \text{ g } Mn(NO_3)_2 \cdot 6H_2O}{X \text{ g } Mn(NO_3)_2 \cdot 6H_2O + 10.00 \text{ g } H_2O} = \frac{0.25 \text{ g } Mn(NO_3)_2 \cdot 6H_2O}{\text{g soln}}$$

$$0.25 * X + 0.25 * 10.00 = X$$

$$0.25 * 10.00 = X - 0.25 * X$$

$$2.5 = 0.75 * X$$

$$X = 3.33 \text{ g } Mn(NO_3)_2 \cdot 6H_2O$$

Therefore, 3.33 grams $Mn(NO_3)_2 \cdot 6H_2O$ was added to 10.00 grams of water to make a twenty-five weight percent $Mn(NO_3)_2 \cdot 6H_2O$ solution which in turn yields a seven weight percent MnO_2 sample on Al_2O_3. To make the calculations simple, ten grams of Al_2O_3 were used. The sample was dried in an oven on the assumption that $Mn(NO_3)_2 \cdot 6H_2O$ converts into MnO_2 with drying.

Y = grams of solution used in the sample

$$Y \text{ g soln} * \frac{0.25 \text{ g } Mn(NO_3)_2 \cdot 6H_2O}{\text{g soln}} * \frac{1 \text{ mol } Mn(NO_3) \cdot 6H_2O_2}{287.04 \text{ g } Mn(NO_3)_2 \cdot 6H_2O} *$$

$$\frac{1 \text{ mol } MnO_2}{1 \text{ mol } Mn(NO_3)_2 \cdot 6H_2O} * \frac{86.94 \text{ g } MnO_2}{\text{mol } MnO_2} = 7.572E\text{-}02 * Y \text{ g } MnO_2$$

A seven weight percent MnO_2 sample was desired. Therefore, the amount of solution added to ten grams of Al_2O_3 could be determined.

$$\frac{7.572E\text{-}02 \cdot Y \text{ g } MnO_2}{7.572E\text{-}02 \cdot Y \text{ g } MnO_2 + 10 \text{ g } Al_2O_3} = \frac{0.07 \text{ g } MnO2}{\text{g dry sample}}$$

where g sample = g MnO_2 + g Al_2O_3

$0.07 * 7.572E\text{-}02 * Y + 0.07 * 10 = 7.572E\text{-}02 * Y$

$0.07 * 10 = 7.572E\text{-}02 * Y - 0.07 * 7.572E\text{-}02 * Y$

$0.7 = 7.042E\text{-}02 * Y$

$Y = 9.94$ g soln

Therefore, 9.94 grams of solution should be added to 10 grams of Al_2O_3 to produce a seven weight percent MnO_2 sample.

Calculations for Actual Weight Percent MnO_2 on Al_2O_3

The calculations used to determine the actual weight percent MnO_2 on Al_2O_3 follow. First, the weight percentage $Mn(NO_3)_2$ in the $Mn(NO_3)_2 \cdot 6H_2O$ solution were determined.

$$\frac{3.33 \text{ g } Mn(NO_3)_2 \cdot 6H_2O}{3.33 \text{ g } Mn(NO_3)_2 \cdot 6H_2O + 10.00 \text{ g } H_2O} = \frac{0.25 \text{ g } Mn(NO_3)_2 \cdot 6H_2O}{\text{g solution}}$$

$$= 25 \text{ wt \% } Mn(NO_3)_2 \cdot 6H_2O$$

where g soln = g $Mn(NO_3)_2 \cdot 6H_2O$ + g H_2O

Next, the amount of $Mn(NO_3)_2 \cdot 6H_2O$ used was calculated.

$$6.19 \text{ g solution} * \frac{0.25 \text{ g } Mn(NO_3)_2 \cdot 6H_2O}{1.00 \text{ g solution}} = 1.55 \text{ g } Mn(NO_3)_2 \cdot 6H_2O$$

$$1.55 \text{ g } Mn(NO_3)_2 \cdot 6H_2O * \frac{1 \text{ mol } Mn(NO_3)_2 \cdot 6H_2O}{287.04 \text{ g } Mn(NO_3)_2 \cdot 6H_2O}$$

$$= 5.340\text{E-}03 \text{ mole } Mn(NO_3)_2 \cdot 6H_2O$$

It was assumed that during drying $Mn(NO_3)_2$ turned into MnO_2.

5.340E-03 mol $Mn(NO_3)_2$ = 5.340E-03 mol MnO_2 after drying

Moles of MnO_2 was converted to grams and the actual weight percentage MnO_2 was calculated.

$$5.340\text{E-}03 \text{ mol } MnO_2 * \frac{86.94 \text{ g}}{\text{mol}} = 0.46 \text{ g } MnO_2$$

$$\frac{0.46 \text{ g } MnO_2}{0.46 \text{ g } MnO_2 + 10.00 \text{ g } Al_2O_3} = \frac{0.0440 \text{ g } MnO_2}{\text{g dry sample}} = 4.40 \text{ wt \% } MnO_2$$

where g dry sample = g MnO_2 + g Al_2O_3

Calculations To Determine Amount For 7 wt % Na_2SO_4 On Al_2O_3

The calculations used to determine the actual recipe for seven weight percent Na_2SO_4 on Al_2O_3 follow. The calculations were simplified by using ten grams of Al_2O_3. A seven weight percent Na_2SO_4 solution was desired.

X = grams of Na_2SO_4 required

$$\frac{X \text{ g } Na_2SO_4}{X \text{ g } Na_2SO_4 + 10.00 \text{ g } Al_2O_3} = \frac{0.07 \text{ g } Na_2SO_4}{\text{g dry sample}}$$

where g dry sample = g Na_2SO_4 + g Al_2O_3

$0.07 * X + 0.07 * 10.00 = X$

$0.7 = X - 0.07 * X$

$0.7 = 0.93 * X$

$X = 0.75$ g Na_2SO_4

Therefore 0.75 g Na_2SO_4 were added to 10.00 g Al_2O_3 to make a seven weight percent Na_2SO_4 sample.

Calculations To Determine Actual Weight Percent Na_2SO_4 on Al_2O_3

The calculations used to determine the actual weight percent Na_2SO_4 on Al_2O_3 follow:

$$\frac{0.70 \text{ g } Na_2SO_4}{0.70 \text{ g } Na_2SO_4 + 10.00 \text{ g } Al_2O_3} = \frac{0.70 \text{ g } Na_2SO_4}{\text{g dry sample}} = 7.0 \text{ wt \% } Na_2SO_4$$

Calculations To Determine Amount For 7 wt % MnO_2 and 1 wt %$Cu(NO_3)_2$ on Al_2O_3

The calculations to determine the amount for 7 wt % MnO_2 are given above under Calculations To Determine the Amount For 7 wt % MnO_2 on Al_2O_3.

One weight percent $Cu(NO_3)_2$ was then added to this sample.

Z = grams of $Cu(NO_3)_2$ used in sample

$$\frac{Z \text{ g } Cu(NO_3)_2}{Z \text{ g } Cu(NO_3)_2 + 10.00 \text{ g } Al_2O_3 + 1.55 \text{ g } MnO_2} = \frac{0.01 \text{ g } Cu(NO_3)_2}{\text{g dry sample}}$$

where g dry sample = g $Cu(NO_3)_2$ + g Al_2O_3 + g MnO_2

$0.01 * Z + 0.01 * 10.00 + 0.01 * 1.55 = Z$

$0.1 + 1.54E\text{-}02 = Z - 0.01 * Z$

$1.15E\text{-}01 = 0.99 * Z$

$Z = 0.12$ g $Cu(NO_3)_2$

Therefore. 0.12 g $Cu(NO_3)_2$ should be added to 9.96 grams of solution and 10.00 grams of Al_2O_3 to make a 7 wt % MnO_2 and 1 wt %$Cu(NO_3)_2$ on Al_2O_3.

Calculations To Determine Actual Weight Percent MnO_2 and $Cu(NO_3)_2$ on Al_2O_3

The calculations used to determine the actual weight percent manganese oxide were calculated above.

The actual weight percentage is shown below.

$$\frac{0.12 \text{ g } Cu(NO_3)_2}{0.47 \text{ g } MnO_2 + 10.00 \text{ g } Al_2O_3 + 0.12 \text{ g } Cu(NO_3)_2} = \frac{0.0113 \text{ g } Cu(NO_3)_2}{\text{g dry sample}}$$

$$= 1.13 \text{ wt \% } Cu(NO_3)_2$$

Calculations To Determine Amount For 7 wt % $Fe(NO_3)_3$ on Al_2O_3

The calculations used to determine the actual weight percent $Fe(NO_3)_3$ follow.

$$2.00\ g\ Fe(NO_3)_3 \cdot 9H_2O * \frac{1\ mol\ Fe(NO_3)_3 \cdot 9H_2O}{404\ g\ Fe(NO_3)_3} = 4.95E\text{-}03\ mol\ Fe(NO_3)_3$$

$$4.95E\text{-}03\ mol\ Fe(NO_3)_3 * \frac{55.85\ g\ Fe}{1\ mol\ Fe(NO_3)_3} = 0.28\ g\ Fe$$

$$\frac{0.28\ g\ Fe}{0.28\ g\ Fe + 10.00\ g\ Al_2O_3 + 40\ g\ NH_3OH} = \frac{0.0055\ g\ Fe}{g\ dry\ sample} = 0.55\ wt\ \%\ Fe$$

where g dry sample = g Fe + g Al_2O_3 + g NH_3OH

APPENDIX B

GRAPHS

Figure 4

Maghemite Adsorption Efficiencies

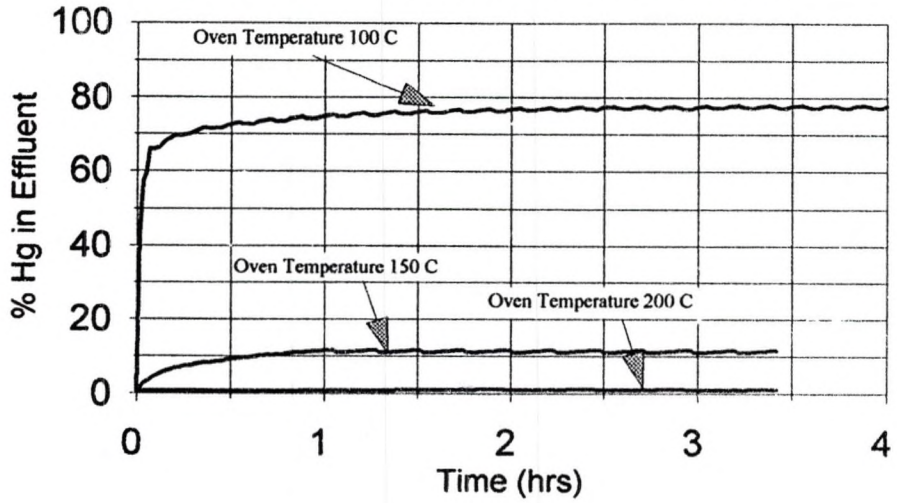

Figure 5

Activation Temperature of Maghemite

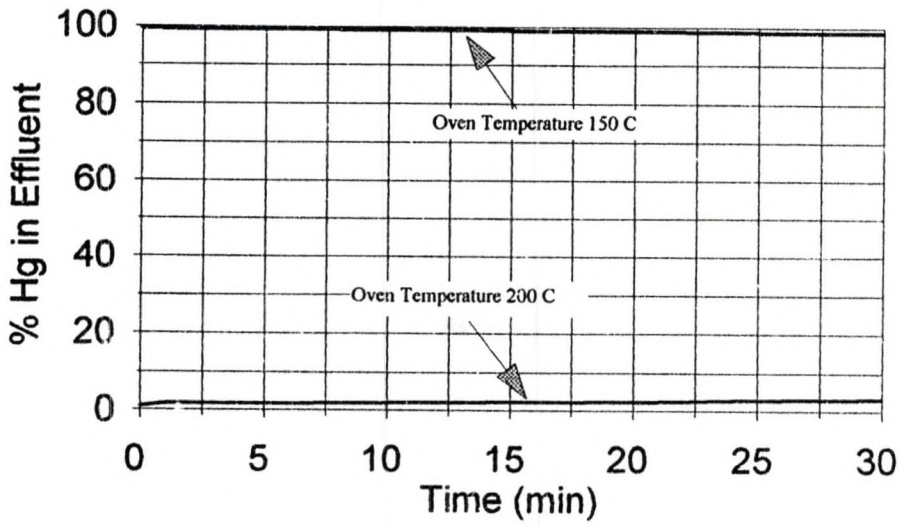

Figure 6

Activation Temperature of Feroxyhyte

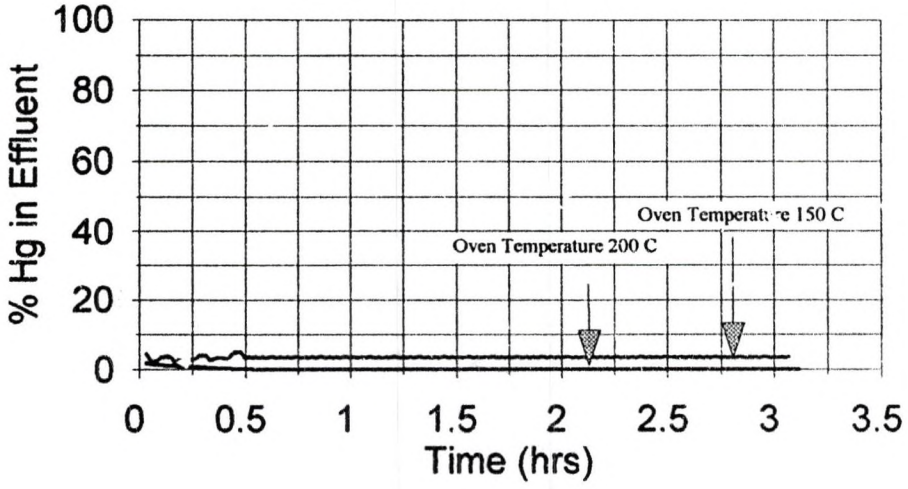

Figure 7

Activation Temp. of Lepidocrocite

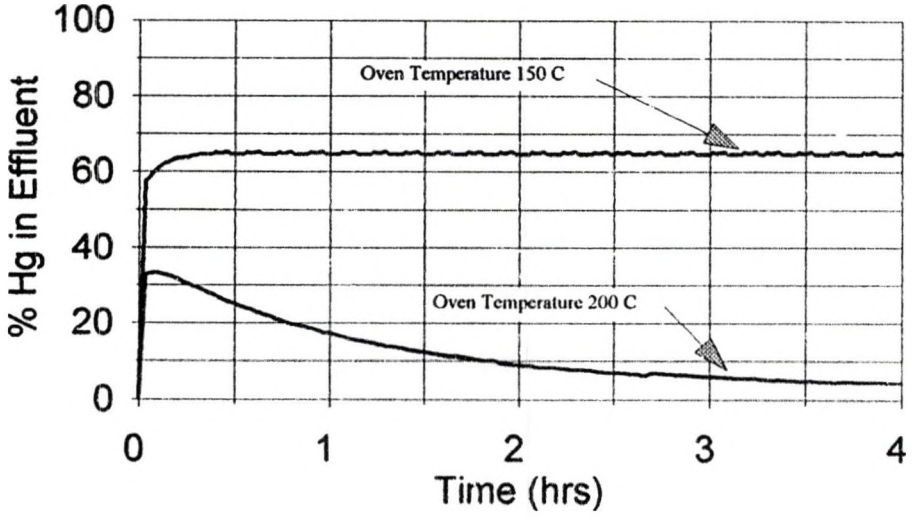

Figure 8

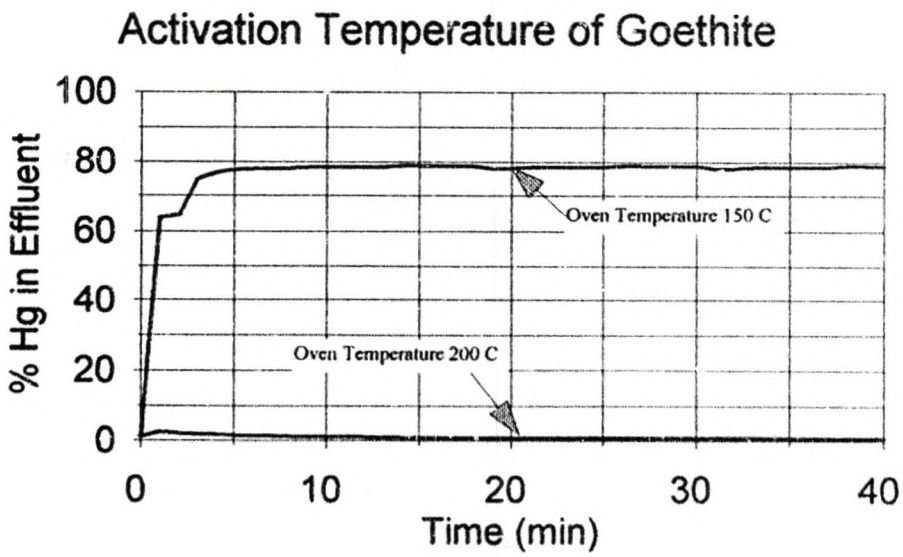

Figure 9

Activation Temp of 2-Line Ferrihydrite

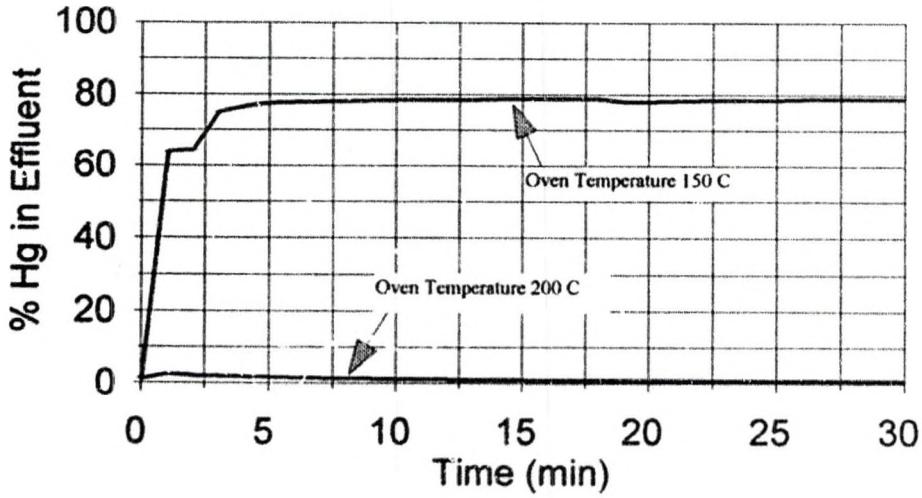

Figure 10

Fe2(SO4)3/Al2O3 Adsorption Efficiency

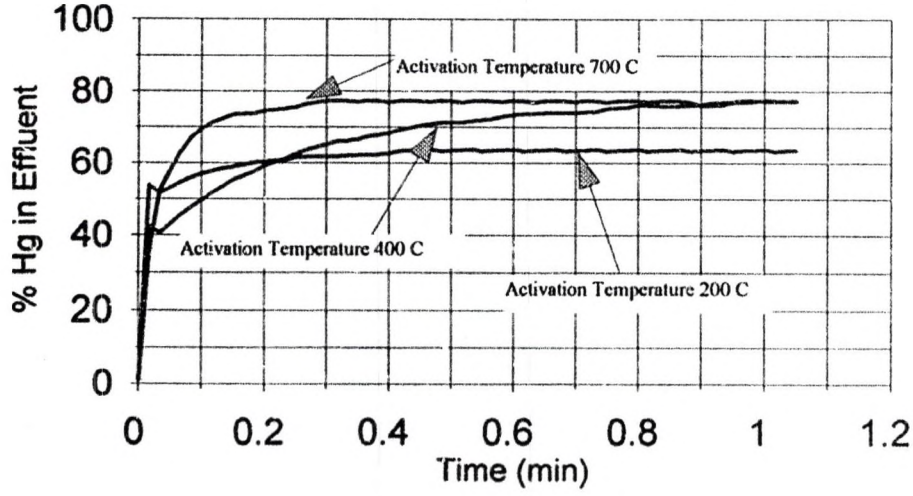

Figure 11

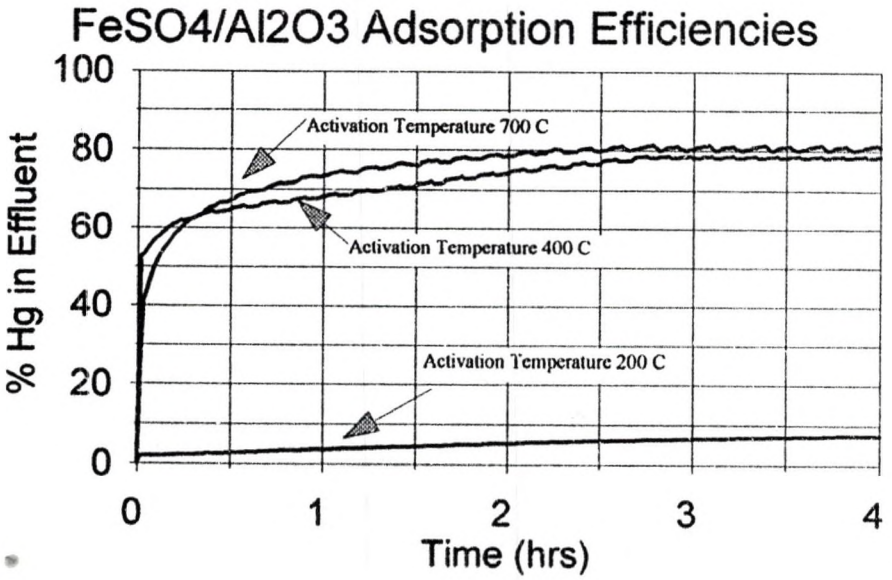

Figure 12

(CH2CO3)2Fe/Al2O3 Adsorption Eff.

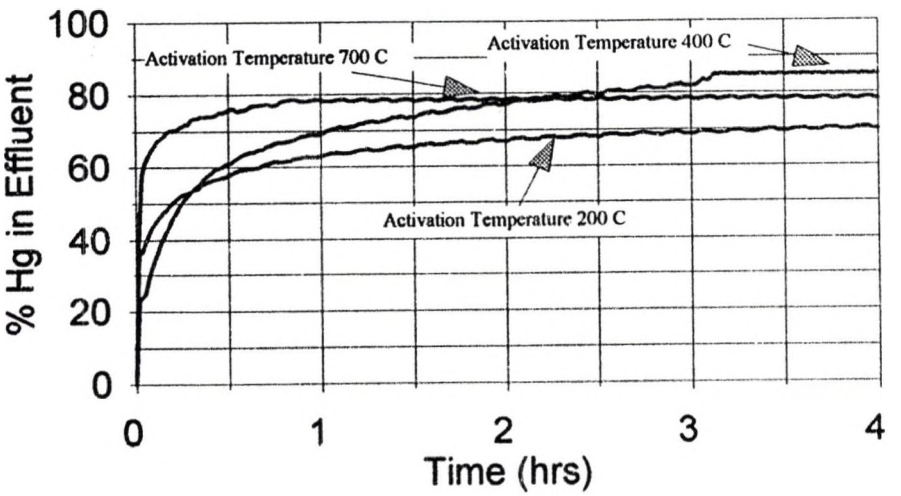

Figure 13

Fe2O3/Al2O3(Method #1)

Adsorption Efficiencies

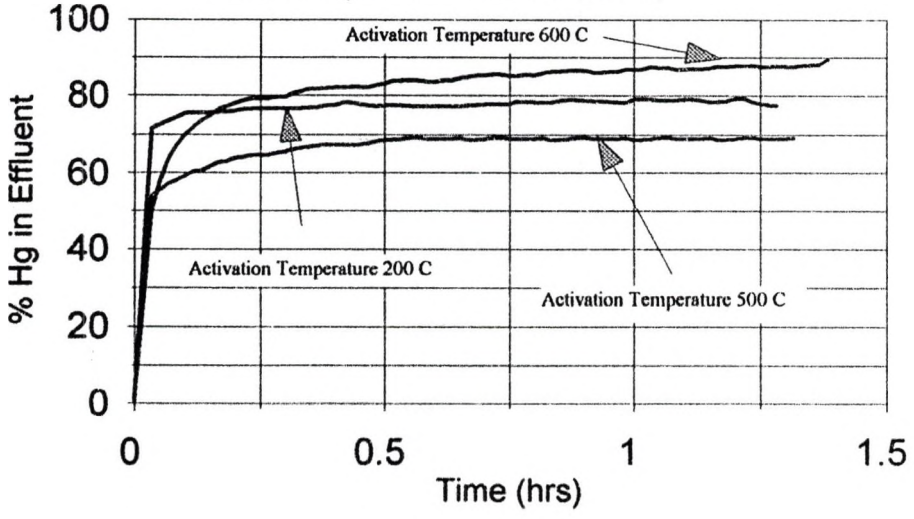

Figure 14

FeOOH/Al2O3(Method #2)

Adsorption Efficiencies

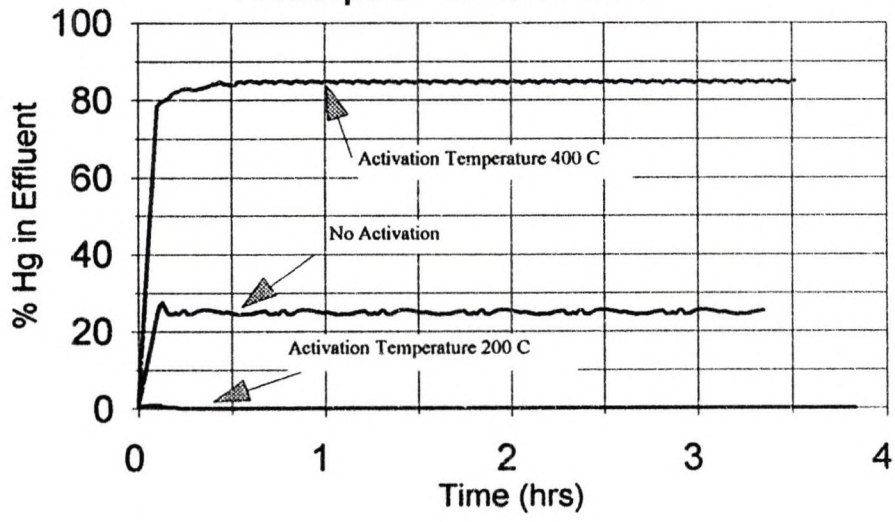

Figure 15

In-Situ Activation

of Mn(C2H3O2)2/Al2O3

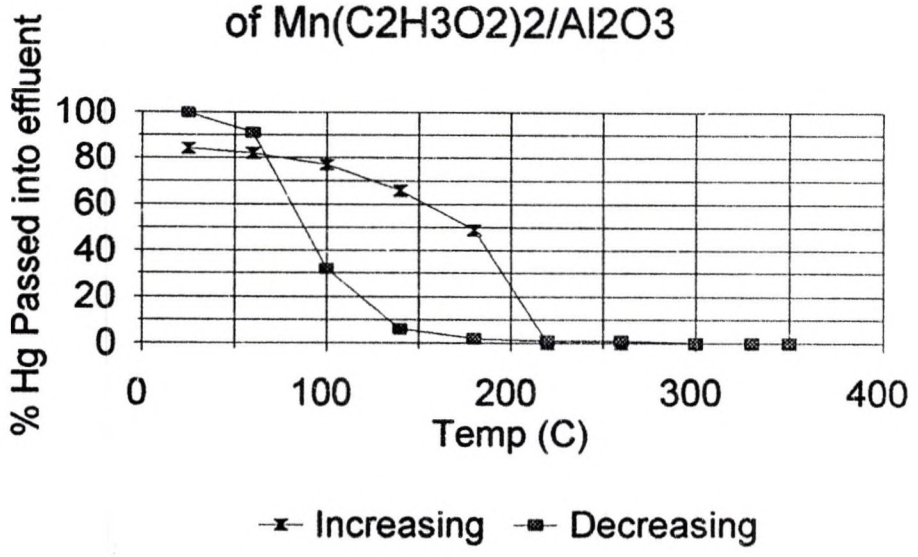

APPENDIX C

INFRARED SPECTROSCOPY

The results of performing infrared spectrophotometry analysis on manganese oxides, iron oxides, and oxides on supports are given in Table 23 which includes the sample name, frequency of major peaks, and the interpretation of those peaks.

Table 23: Infrared Spectrophotometry Results

Sample	Infrared Wavenumber (cm-1)	Interpretation
MnO_2/Al_2O_3	1381	Characteristic of nitrates. No peak was found to correspond to manganese oxide.
Mn_2O_3	647 604 533 510	Unique peaks characteristic to manganese sesquioxide.
MnO_2/carbon	639	Few peaks observed. Carbon does not have significant characteristic peaks.
MnO_2/y-zeolite	Hard to Interpret	Hard to interpret.
MnOOH	2062 2103 1161 1086 587 483	Unique peaks characteristic to manganese oxyhydroxide. No peaks found to correspond to Mn_2O_3 and MnO_2.
$MnSO_4/Al_2O_3$	1146	Characteristic to sulfates.
MnO_2/Al_2O_3 & H_2SO_4	1378 1130	Characteristic to nitrates. Characteristic of aluminum oxide.

Table 50 cont.

$Mn(C_2H_3O_2)_2/Al_2O_3$ (Activ Temp 200)	1429 1555	Characteristic to the acetate.
$Mn(C_2H_3O_2)_2/Al_2O_3$ (Activ Temp 400)	No Significant	Acetate peaks no longer appear.
$KmnO_4$, $KmnO_4$ & Oxalic Acid, $KmnO_4$ & Hydrogen Peroxide	914	Peaks characteristic to potasium permanganate are undistiguishable from the aluminum oxide bands. It is therefore hard to interpret.
Hematite (No Activation)	1385	Characteristic of hematite.
Hematite (Oven Temp 200)	Same as Above	Same as above.
Magnetite (No Activation)	590	Characteristic of magnetite.
Magnetite (Oven Temp 200)	597 1370 1570	Characteristic of magnetite. Characteristic of hematite. The peak was small; therefore, only a small amount of hematite was formed. Formed another compound.
Maghemite (No Activation)	636 1620	Characteristic of maghemite.
Maghemite (Oven Temp 200)	Same as Above	Same as above.
Goethite (No Activation)	790 894 1385	Characteristic of goethite. Characteristic of goethite. Characteristic of hematite.
Goethite (Oven Temp 200)	Same as Above	Same as above.
Lepidocrocite (No Activation)	1018	Characteristic to lepidocrocite.
Lepidocrocite (Oven Temp 200)	644 746 1612	Peaks are characteristic to maghemite.

Table 50 cont.

Ferrihydrite (No Activation)	1128 1626	Both peaks characteristic of ferrihydrite.
Ferrihydrite (Oven Temp 200)	1130 1560 1620	Characteristic to ferrihydrite. Similar structure to maghemite. Characteristic to ferrihydrite.
2-Line Ferrihydrite (No Activation)	654 1347 1513 1622	Peaks are characteristic to 2-line ferrihydrite.
2-Line Ferrihydrite (Oven Temp 200)	Same as Above	Same as above.
Feroxyhyte (No Activation)	533 1334 1558	Characteristic of feroxyhyte.
Feroxyhyte (Oven Temp 200)	533 894 793 1334	 Characteristic of goethite. Characteristic of goethite.
Mn-Fe Goethite (No Activation)	793 900 1380	Characteristic of goethite.
Mn-Fe Goethite (Oven Temp 200)	Same as Above	Characteristic of manganese-iron goethite.
$(C_2H_3O_2)_2Fe/Al_2O_3$ (Oven Temp 200)	1455 1563	Characteristic of acetate.
$(C_2H_3O_2)_2Fe/Al_2O_3$ (Oven Temp 400)	1550	Characteristic of acetate. Peak was smaller; therefore, more acetate decomposed.
$FeCl_3/Al_2C_3$	1620	Characteristic of maghemite.
$Fe_2(SO_4)_3/Al_2O_3$ (Oven Temp 200)	1101 1650	Characteristic of sulfate. Unique peak could be due to sulfate combining with the iron oxide.
$Fe_2(SO_4)_3/Al_2O_3$ (Oven Temp 400)	1641	Unique peak could be due to sulfate combining with the iron oxide.

Table 50 cont.

$FeSO_4/Al_2O_3$ (Oven Temp 200)	1370	This peak is not characteristic of sulfate and therefore could be due to iron oxide.
$FeSO_4/Al_2O_3$ (Oven Temp 400)	No Significant	No significant peaks.
Fe_2O_3/Al_2O_3 (Oven Temp 200)	855 1360	Characteristic to aluminum oxide. Characteristic to nitrate.
$FeOOH/Al_2O_3$ (Oven Temp 200)	1146 1380 1405 1652	Characteristic of ferrihydrite. haracteristic of nitrate. Characteristic of nitrate. Characteristic of hydroxyoxide.

REFERENCES

Barrer, R.M. and Whiteman, J.L., "Mercury Uptake in Various Cationic Forms of Several Zeolites," Journal of American Chemical Society, 1967, pp. 19-25.

Behrens, G.P. and Chu, P., "Variability Analysis for Measurements of Trace Substances in Power Plant Stack Gas," Presented at Air & Waste Management Association 87th Annual Meeting & Exhibition, Cincinnati, OH, Vol. 13, June 19-24, 1994, pp. 1-16.

Bergstrom, J.G.T., "Mercury Behavior in Flue Gases," Waste Management & Research, Vol. 4, 1986, pp.57-64.

Carroll, G.J. and Thurnau, R.C., "Control of Mercury Emissions from Hazardous Waste Incineration," Presented at 87th Annual Meeting & Exhibition, Cincinnati, OH, Vol. 13, June 19-24, 1994, pp.1-16.

Caruana, C.M., "Mercury Pollution: Seeking a Quicksilver Lining," Chemical Engineering Progress, Jan. 1996, pp. 10-16.

Cavallaro, S., Bertuccio, N., Antonucci, P., and Giordano, N., "Mercury Removal from Waste Gases by Manganese Oxide Acceptors," Journal of Catalysts, Vol. 93, 1982, pp. 337-348.

Clarke, L.B., "The Fate of Trace Elements During Coal Combustion and Gasification: An Overview," Fuel, Vol. 72, No. 6, 1993, pp. 731-736.

Constantinou, E.. Gerath, M. Mitchell, D., Seigneur, C. and Levin, L., "Mercury From Power Plants: A Probablistic Approach To The Evaluation of Potential Health Risks," Water, Air, and Soil Pollution, Vol. 80, 1995, pp. 1129-1138.

Dvonch, J. T., Vette, A.F., Keeler, G.J., Evans, G. and Stevens, R., "An Intensive Multi-Site Pilot Study Investigating Atmospheric Mercury In Broward County, Florida, "Water, Air, and Soil Pollution, Vol. 80, 1995, pp. 179-188.

Ebbing, D.D. and Wrighton, M.S., General Chemistry, Houghton Mifflin Company, Boston, MA, 1990.

Facemire, C. Augspurger, T., Bateman, D., Brim, M., Conzelmann, P., Delchamps, S., Douglas, E., Inmon, L., Looney, K., Lopez, F., Masson, G., Morrison, D., Morse, N., and Robison, A., "Impacts of Mercury Contamination In The Southeastern United States," Water, Air, and Soil Pollution, Vol. 80, 1995, pp. 923-926.

Fang, S.C., "Sorption and Transformation of Mercury Vapor by Dry Soil," Environmental Science & Technology, Vol. 12, No. 3, March 1978, pp. 285-288.

Hall, B., Schager, P. and Lindqvist, O., "Chemical Reactions of Mercury In Combustion Flue Gases," Water, Air, and Soil Pollution, Vol. 56, 1991, pp. 3-14.

Lancia, A., Musmarra, D., Pepe, F., and Volpicelli, G., "Adsorption of Mercuric Chloride Vapours from Incinerator Flue Gases on Calcium Hydroxide Particles," Combustion Science and Technology, Vol. 93, 1993, pp. 277-289.

Licata, A., Babu, M., and Nethe, L., "An Economic Alternative to Controlling Acid Gases, Mercury and Dioxin From MWCS," Presented at Air & Waste Management 87th Annual Meeting, June 19-24, 1994, Cincinnati, OH, pp.1-21.

Metzger, M. And Braun, H., "In-Situ Mercury Speciation In Flue Gas By Liquid and Solid Sorption Systems," Chemosphere, Vol. 16, No. 4, 1987, pp. 821-832.

Mojtahedi, W. and Mroueh, U., "Trace Element Removal From Hot Flue Gases," Technical Research Center of Finland, Research Reports 663, 1989, pp. 8 -18.

Moore, T.E., Ellis, M., and Selwood, P.W., "Solid Hydroxides of Manganese," Vol. 72, Feb. 1950, pp. 856-866.

Morency, R., Srinivasachar, S., Lemieux, P.M., Ryan, J.V., and Meckes, M.C., "Control of Trace Metals Species in Combustion Systems," Presented Air & Waste Management 87th Annual Meeting & Exhibition, Cincinnati, OH, Vol. 6A, June 19-24, 1994, pp. 1-16.

Moretti, C. J. and Olson, E., "Geotechnical/Geochemical Characterization of Advanced Coal Process Waste Streams: Task 2 Report," Universal Fuel Development Associates, Inc., September 1992, pp. 1-29.

Nguyen, X.T., " Adsorbents for Mercury Vapor Removal," Journal of the Air Pollution Control Association, Vol. 29, No. 3, March 1979, pp. 235-237.

Otani, Y., Emi, H., Kanaoka, C., and Matsiu, S., "Behavior of Metal Mercury in Gases," Environmental Science Technology, Vol. 18, No. 10, 1984, pp. 793-796.

Otani, Y., Kanaoka, C., Usui, C., Matsui, S., and Emi, H., "Adsorption of Mercury Vapor on Particles," Environmental Science Technology, Vol. 20, No. 7, 1986, pp. 735-738.

Prestbo, E.M. and Bloom, N.S., "Mercury Speciation Adsorption (MESA) Methodology, Artifacts, Intercomparison, and Atmospheric Implications," Water, Air, and Soil Pollution, Vol. 80, 1995, pp. 145-158.

Samdani, G.S., "Zeolites Capture Mercury and Dioxins From Incinerator Flue Gas," Chemical Engineering, Vol. 101, No. 10, 1994, p. 19.

Sappey, A.D., Wilson, K.G., Schlager, R.J., Anderson, G.L., and Jackson, D.W., "A Continuous Emissions Monitor For Total, Elemental, and Total Speciated Mercury," Preparation Paper, American Chemical Society Division of Fuel Chemistry, Vol. 40, No. 4, 1995, pp. 818-822.

Schlager, R. J. Durham, M.D., and Marmaro, R.W., "Monitoring Total and Speciated Mercury by Ultraviolet Absorption Spectroscopy," Process Control and Quality, Vol. 7, No. 2, 1995, pp. 97-100.

Schwertmann, U. and Cornell, R.M., Iron Oxides in the Laboratory, VCH Publishers, Inc., New York, NY, 1991.

Shell, K.J. and Anderson-Carnahan, L., "A Multi-Media Approach To Permitting Mercury Releases From Coal-Fired Power Plants," Water, Air, and Soil Pollution, Vol. 80, 1995, pp. 1161-1170.

U.S. Department of Energy, "A Comprehensive Assessment form Coal-Fired Power Plants: Phase 1 Results," Pittsburgh Enegy Technology Center, U.S. Department of Energy, September 1996.

Weekman, V.W. and Yan, T.Y., "Regenerative Mercury Removal Process," 1995, Pennsylvania, USA, Application # 20943, Patent #5419884.

Von Burg, R., "Toxicology Update: Inorganic Mercury," Journal of Applied Toxicology," Vol, 15, No. 6, 1995, pp. 483-493.

Yan, T.Y., "A Novel Process for Hg Removal from Gases," Ind. Engineering Chemical Research, Vol. 33, 1994, pp. 3010-3014.

Zeugin, L.B., "Air Toxics Issues for Power Production," Presented at 87th Annual Meeting & Exhibition, Cincinnati, OH, Vol. 4A, June 19-24, 1994.